EFFECTS OF FERRATE(VI) AND ENGINEERED NANOMATERIALS ON FORMATION AND TOXICITY OF DISINFECTION BYPRODUCTS IN SYNTHETIC DRINKING WATER SAMPLES

A Dissertation

by

COLE MATTHEW GRAY

Submitted to the Office of Graduate and Professional Studies of
Texas A&M University
in partial fulfillment of the requirements for the degree of

DOCTOR OF PUBLIC HEALTH

Chair of Committee,	Leslie Cizmas
Committee Members,	Thomas McDonald
	Itza Mendoza-Sanchez
	Daikwon Han
Head of Department,	Mark Benden

May 2020

Major Subject: Environmental Health

ABSTRACT

The role of different disinfectants [chlorination and ferrate(VI)] and microcontaminant (TiO_2 and ZnO nanoparticles) regimens on the formation of nine disinfection byproducts (DBPs) in synthetic drinking water samples and their subsequent cytotoxic effects were assessed in depth. Specifically, water samples were chemically analyzed with gas chromatography/mass spectrometry (GC/MS), while their concentrated extracts underwent a battery of cellular assays (chronic cytotoxicity, viability, ROS generation, and autophagy) using one mammalian cell line (CHO-K1) and four human cell lines (CaCo-2, HEK293, GES-1, and FHC). Chemical analysis results indicated that that only waters disinfected with chlorine produced any concentration of the examined DBPs. Data from the chronic cytotoxicity assays showed that no sample extracts produced a significant change in cytotoxicity levels among CHO-K1 cells as compared to control samples at corresponding dilution levels. Among CaCo-2 cells, extracts from samples dosed with TiO_2 and ZnO at the 0.8x dilution level showed significant increases in cytotoxicity compared to control samples at the corresponding dilution level. The cell viability and ROS assays showed that extracts from waters disinfected with ferrate(VI) were significantly less toxic to HEK293 cells compared to extracts from waters disinfected by chlorine, and produced a significant increase in ROS generation among GES-1 cells. Extracts from ZnO-dosed waters produced a significant increase in cell density and ROS generation among GES-1 and FHC cell lines, respectively. Lastly, it was shown that none of the extracts enhanced autophagic vacuole (AVO) accumulation

among HEK293 cells, indicating low levels of cellular stress. Overall, these findings highlight various ways by which disinfectants and emerging contaminants such as NPs can influence the production and cytotoxic effects of DBP mixtures.

DEDICATION

This work is dedicated to my mother, father, and brother for their love and encouragement over all these years.

ACKNOWLEDGEMENTS

I would like to extend my gratitude to my advisor and committee chair, Dr. Leslie Cizmas for her unwavering patience, guidance, and support over the course of this research project and my doctoral degree. My thanks, also, to my committee members, Dr. McDonald, Dr. Mendoza, and Dr. Han for their contributions to the completion of this research project. I also thank Dr. Sharma for his substantial support and advice during my research.

Last, I'd like to thank my colleagues and the department faculty and staff at Texas A&M and the School of Public Health for adding so much to my educational experience.

CONTRIBUTORS AND FUNDING SOURCES

Contributors

This work was supervised by a dissertation committee consisting of Professors Leslie Cizmas, Thomas McDonald, and Itza Mendoza of the Department of Environmental and Occupational Health and Professor Daikwon Han of the Department of Epidemiology and Biostatistics. Dr. Virender Sharma was also extremely supportive in providing ideas, advice and ferrate for my research.

The chemical analysis data for sections 2.3.1, 3.3.1, and 4.3.1 were provided by Alexin Analytical Laboratories, Tigard, OR.

Data for section 4.0 were generated with the generous collaboration and advice of Professor Bing Yan, Professor Shumei Zhai, and Hainan Sun of Jinan University, Guangzhou, P.R. China.

All other work for the dissertation was completed by the student independently.

Funding Sources

This graduate study was supported by a fellowship from Texas A&M University and dissertation research grants from the Center for Translational Environmental Health Research (CTEHR) and the School of Public Health Research Enhancement and Development Initiative (REDI) Fund.

NOMENCLATURE

AVO	Autophagic vacuole
CaCo-2	Colorectal adenocarcinoma cells
CF	Concentration factor
CHO	Chinese hamster ovary cells
CNT	Carbon Nanotubes
DBP	Disinfection byproduct
DHAAs	Dihaloacetic acids
DHANs	Dihaloacetonitriles
ENM	Engineered Nanomaterials
Fe(VI)	Ferrate(VI)
GC/MS	Gas chromatography/mass spectrometry
HAA	Haloacetic acid
HAA5	Total of five regulated haloacetic acids comprising of monochloroacetic acid, trichloroacetic acid, dichloroacetic acid, monobromoacetic acid, and dibromoacetic acid.
HAN	Haloacetonitrile
HKs	Haloketones
KI	Potassium iodide
N-DBP	Nitrogenous disinfection byproduct
NaBr	Sodium bromide
NDMA	N-nitrosodimethylamine
NOM	Natural organic matter

NP	Nanoparticle
SPE	Solid phase extraction
THAAs	trihaloacetic acids (THAAs)
THM	Trihalomethanes
TTHM	Total of four regulated trihalomethanes including trichloromethane (chloroform), dibromochloromethane, bromodichloromethane, and tribromomethane (bromoform).
TiO_2 NPs	Titanium dioxide nanoparticles
TiO_2/PC	Titanium dioxide photocatalysis
TiO_2/PEC	Titanium dioxide photoelectrocatalysis
TOX	Total organic halogen
ZnO NPs	Zinc oxide nanoparticles

TABLE OF CONTENTS

Page

ABSTRACT ii

DEDICATION iv

ACKNOWLEDGEMENTS v

CONTRIBUTORS AND FUNDING SOURCES vi

NOMENCLATURE vii

TABLE OF CONTENTS ix

LIST OF FIGURES xii

LIST OF TABLES xiv

1. INTRODUCTION 1

1.1. Problem Statement 1
1.2. Present State of Knowledge 3
1.3. References 6

2. A MULTI-STEP APPROACH TO ASSESSING AND COMPARING DISINFECTION BYPRODUCT FORMATION AND CYTOTOXICITY FOLLOWING CHLORINATION OR FERRATE(VI) DISINFECTION 16

2.1. Introduction 16
2.2. Materials & Methods 19
    2.2.1. Chemicals & Reagents 19
    2.2.2. Preparation of Water Samples 19
    2.2.3. Concentration of the Extract 20
    2.2.4. Chemical Analyses 21
    2.2.5. Cell Lines 22
        2.2.5.1. Chinese Hamster Ovary Cells 22
        2.2.5.2 Human Colorectal Adenocarcinoma Cells 23
    2.2.6. Chronic Cell Cytotoxicity Assays 23
    2.2.7. Statistical Analyses 24
2.3. Results 24

2.3.1. Chemical Analysis....24
2.3.2. Chronic Cell Cytotoxicity Assays....27
2.3.2.1. CHO-K1 Cellular Assay....27
2.3.2.2. CaCo-2 Cellular Assay....27
2.4. Conclusions....28
2.5. References....30

3. A MULTI-STEP APPROACH TO ASSESSING DISINFECTION BYPRODUCT FORMATION AND CYTOTOXICITY OF SYNTHETIC DRINKING WATERS DOSED WITH TITANIUM DIOXIDE (TiO_2) OR ZINC OXIDE (ZnO) NANOPARTICLES....33

3.1. Introduction....33
3.2. Materials & Methods....34
3.2.1. Chemicals & Reagents....34
3.2.2. Preparation of Nanoparticle Water Samples....35
3.2.3. Concentration of the Extract....36
3.2.4. Chemical Analyses....36
3.2.5. Cell Lines....36
3.2.5.1. Chinese Hamster Ovary Cells....36
3.2.5.2 Human Colon Adenocarcinoma Cells....37
3.2.6. Cytotoxicity Bioassays....37
3.2.7. Statistical Analyses....38
3.3. Results....38
3.3.1. Chemical Analysis....38
3.3.2. Chronic Cell Cytotoxicity Assays....39
3.3.2.1. CHO-K1 Cellular Assay....39
3.3.2.2. CaCo-2 Cellular Assay....40
3.4. Conclusions....42
3.5. References....44

4. ASSESSING AND COMPARING HUMAN BIOASSAY SENSITIVITIES FOR CYTOTOXICITY, ROS GENERATION, AND AUTOPHAGY FOLLOWING EXPOSURE TO COMPLEX DISINFECTION BYPRODUCT MIXTURES....46

4.1. Introduction....46
4.2. Materials & Methods....49
4.2.1. Chemicals & Reagents....49
4.2.2. Preparation of Water Samples....50
4.2.3. Concentration of the Extract....50
4.2.4. Chemical Analyses....50
4.2.5. Human Cell Lines....51
4.2.6. Cell Viability Assay....51
4.2.7. Reactive Oxygen Species (ROS) Generation Assay....52

4.2.8. Autophagy Assay 53
4.2.9. Statistical Analyses 53
4.3. Results 54
4.3.1. Chemical Analysis 54
4.3.2. Cell Viability Assay 54
4.3.3. ROS Generation Assay 58
4.3.4. Autophagy Assay 63
4.4. Conclusions 64
4.5. References 66

5. CONCLUSIONS 71

APPENDIX A FIGURES 75

APPENDIX B TABLES 92

LIST OF FIGURES

Page

Figure 2.1 Chemical Analysis Graph: Effect of Disinfectants on Trihalomethane Concentrations. 25

Figure 2.2 Chemical Analysis Graph: Effect of Disinfectants on Haloacetic Acid Concentrations. 26

Figure 3.1 Chronic CaCo-2 Cell Cytotoxicity: Assay Results for Drinking Water Samples Dosed with Nanoparticles. 41

Figure 4.1 Cell Viability Assay: HEK293 Cells Disinfectant Extracts. 55

Figure 4.2 Cell Viability Assay: HEK293 Cells Nanoparticle Extracts. 56

Figure 4.3 ROS Assay: GES-1 Cells Disinfectant Extracts. 59

Figure 4.4 ROS Assay: GES-1 Nanoparticle Extracts. 60

Figure 4.5 ROS Assay: FHC Cells Nanoparticle Extracts. 61

Figure A.1 Chronic CHO Cell Cytotoxicity: Assay Results for Samples Treated with Different Disinfectants. 75

Figure A.2 Chronic CaCo-2 Cell Cytotoxicity: Assay Results for Samples Treated with Different Disinfectants. 76

Figure A.3 Chemical Analysis Graph: Effect of Nanoparticles on Trihalomethane Concentrations. 77

Figure A.4 Chemical Analysis Graph: Effect of Nanoparticles on Haloacetic Acid Concentrations. 78

Figure A.5 Chronic CHO Cell Cytotoxicity: Assay Results for Samples Treated with Nanoparticles. 79

Figure A.6 Cell Viability Assay: GES-1 Cells Disinfectant Extracts. 80

Figure A.7 Cell Viability Assay: GES-1 Cells Nanoparticle Extracts. 81

Figure A.8 Cell Viability Assay: FHC Cells Disinfectant Extracts. 82

Figure A.9 Cell Viability Assay: FHC Cells Nanoparticle Extracts. 83

Figure A.10 ROS Assay: HEK293 Cells Disinfectant Extracts. 84

Figure A.11 ROS Assay: HEK293 Cells Nanopaticle Extracts. 85

Figure A.12 ROS Assay: FHC Cells Disinfectant Extracts. 86

Figure A.13 Fixed HEK293 cells with florescent markers that identify the cytoplasmic sites of AVO accumulation after exposure to extracts from chlorinated drinking water. 87

Figure A.14 Fixed HEK293 cells with florescent markers that identify the cytoplasmic sites of AVO accumulation after exposure to extracts from drinking water disinfected with 28.2 uM ferrate(VI). 88

Figure A.15 Fixed HEK293 cells with florescent markers that identify the cytoplasmic sites of AVO accumulation after exposure to extracts from drinking water disinfected with 100 uM ferrate(VI). 89

Figure A.16 Fixed HEK293 cells with florescent markers that identify the cytoplasmic sites of AVO accumulation after exposure to extracts from drinking water dosed with TiO_2. 90

Figure A.17 Fixed HEK293 cells with florescent markers that identify the cytoplasmic sites of AVO accumulation after exposure to extracts from drinking water dosed with ZnO. 91

LIST OF TABLES

Page

Table 1 Chemical/Compound Information. 92

Table 2 Autophagy Assay Results. 93

1. INTRODUCTION

1.1. Problem Statement

Conventional chemical disinfection methods have provided a vital safeguard against waterborne pathogens for over a century (Sedlak, 2011). These processes, unfortunately, also lead to the formation of disinfection byproducts (DBPs). Epidemiological studies have associated DBPs with a variety of human health effects, including cancer of the bladder, colon, and rectum, asthma, adverse reproductive effects and pregnancy outcomes (Richardson, 2015; Villanueva, 2006). Hundreds of DBPs can result from interactions between aqueous chlorine and common source water constituents such as natural organic matter (NOM), halides, and various anthropogenic contaminants. Both municipal and centralized wastewater treatment plants have difficulty eliminating these precursors, so DBPs are present throughout water distribution systems. These may be inhaled or ingested by regular water consumption, showering, bathing, or swimming (Krasner, 2006; Richardson, 2015; Villanueva, 2006; Warner, 2013). The most commonly detected class of volatile DBPs are trihalomethanes [THMs (e.g., bromoform ($CHBr_3$), dibromochloromethane ($CHClBr_2$), chloroform and trichloromethane ($CHCl_3$)]. Trihalomethanes also include haloketones, halophenols, and haloacetonitriles (HANs) (Liu, 2015). The most commonly detected non-volatile class of DBPs are the haloacetic acids [HAAs (e.g., dibromoacetic acid ($C_2H_2Br_2O_2$), monochloroacetic acid ($ClCH_2CO_2H$), monobromoacetic acid ($C_2H_3BrO_2$), dichloroacetic acid ($C_2H_2Cl_2O_2$), and trichloroacetic acid ($C_2HCl_3O_2$)] (Stalter, 2016).

The formation of DBPs following chlorination of drinking water is an important health concern, and there is a corresponding need to develop water disinfection methods that reduce overall DBP generation. Chloramination was widely implemented toward this goal, since monochloramine (NH_2Cl) depresses the formation of regulated THMs and HAAs. It was quickly discovered, however, that during chloramination the reactive products of monochloromine [i.e. hypochlorous acid (HOCl)] can oxidize bromide in source waters to form various unregulated brominated DBPs (Br-DBPs) (Zhai, 2014). It has also been shown that more than 70% of the total organic halogen (TOX) formed by chloramines cannot be attributed to any identified DBPs (Hua & Reckhow, 2007; Diehl, 2000). This value exceeds chlorination where 50% of TOX could not be attributed (Richardson, 2003; 2015).

Engineered nanomaterials (e.g. metallic, adsorbents, filter media, and reactive agents) present another important public health concern in regard to DBP formation. For instance, the carbon nanotube (CNT) fullerene (C60) was shown to have potential uses as an adsorbent in drinking water. Upon oxidation during chemical disinfection, however, C60 was reported to serve as the precursor of halogenated DBPs, including THMs, HAAs and HNMs (Verdugo *et al.*, 2014, 2016). Another example includes the use of titanium dioxide photocatalysis (TiO_2/PC) and titanium dioxide photoelectrocatalysis (TiO_2/PEC) to reduce DBP formation in drinking waters. An investigation by Richardson *et al.* (1996) identified 3-methyl-2, 4- hexanedione, Cl-DBPs, Br-DBPs, and bromate as various DBPs resulting from the TiO_2/PC treatment.

As technological innovations cause new disinfectants and more anthropogenic contaminants to emerge, it is important to continually assess how novel compounds might contribute to the formation and toxicity of DBPs in potable water resources in order to safely navigate potential negative impacts on public health.

1.2. Present State of Knowledge

Previous research has focused heavily on identifying specific DBPs, assessing their toxicity, and delineating the mechanisms behind DBP toxicity. Nearly 700 DBPs have been characterized so far, displaying a range of relative toxicities and toxic mechanisms when compared across species (Richardson & Postigo, 2018; Yang & Zhang, 2016). HAAs, for instance, are known to induce oxidative stress by a variety of pathways [i.e. the ataxia telangiectasia mutated gene (ATM); mitogen-activated protein kinases (MAPK); cellular tumor antigen p53 (p53); ataxia telangiectasia and Rad3 related genes (ATR), and nuclear factor erythroid 2 (NF-E2)-related factor 2 (Nrf2)] (Attene-Ramos *et al.*, 2010; Pals *et al.*, 2013; Plewa *et al.*, 2010; Prochazka *et al.*, 2015). Oxidative stress also plays an important role in THM-induced cellular injury by inducing lipid peroxidation, oxidative DNA damage, as well as metabolic and inflammatory responses, which, in turn, may lead to necrotic or apoptotic processes (Das *et al.*, 2013; Faustino-Rocha, 2016). For relative toxicities, it was found that haloacetonitriles (HANs), for example, are more toxic than the DBPs that are currently regulated (i.e., HAAs and THMs) (Muellner, 2007). Nitrogenous DBPs (N-DBPs) that are often formed during chloramination are of concern as well because certain N-DBPs such as N-nitrosodimethylamine (NDMA) are far more genotoxic than chlorinated DBPs (Cl-

DBPs) (Mitch, 2003; Plewa, 2004; Richardson & Fasano, 2008). Differences in toxicity also exist between individual DBPs belonging to the same species. For instance, when ranking DBPs belonging to the THM species for chronic CHO cell cytotoxicity, bromoform is found to be far more cytotoxic than chloroform, while chloroform is more cytotoxic than bromodichloromethane (BDCM) (Plewa, 2010). The toxicity of a DBP is also contingent on the amount present in finished sources of drinking water, which is dictated by their rate of formation during the disinfection process. The formation rate of DBPs is influenced by water type (e.g. tap water, pool water, recycled waters), disinfectant type (e.g., chlorination, chloramination, UV), and prevailing environmental conditions (e.g., pH, salinity, dissolved organic carbon). The degree of toxicity exerted by a DBP can also change greatly depending upon the target organism or assay tissue (e.g., humans, hamsters, rats, fish) under examination (Richardson, 2015).

There have, in turn, been numerous investigations into the mechanisms by which DBPs are formed and their associations with specific disinfectant technologies (Bond, 2014; Chen, 2010; Golea, 2017; Hong, 2013; Hung, 2017; Warner, 2013). Even so, there is still relatively little research examining the toxicity of complex DBP mixtures (i.e. amalgams of unspecified DBPs generated under natural conditions), or the role of emerging disinfectant technologies and anthropogenic contaminants in their formation and toxicity in drinking water. One such technology of interest is the compound ferrate(VI) [(FeVI), (FeO_4^{2-})]. Fe(VI) is a strong oxidant and hydroxylating agent which shows promise as a comprehensive disinfectant for both wastewater and the production of potable drinking water (Jiang, 2014; Sharma, 2013). Unlike chlorine, chloramine, and

ozone, Fe(VI) only produces non-toxic iron(III) [Fe(III)] during the disinfection process which further aids in its ability to coagulate contaminants (Sharma, 2015). It also has the ability to oxidize emerging contaminants like estrogens, bisphenol-A, and pharmaceuticals present in water (Sharma, 2013; Sharma, 2015). Ferrate(VI), however, remains at the initial stages of development as an alternative disinfection process, and its potential interactions with DBP precursors (including DBP formation) are largely unknown.

Nanoparticles (NPs) are an emerging anthropogenic contaminant of interest in regard to DBP formation. NPs are produced for an increasingly wide variety of applications (e.g. industrial, biomedical, and consumer products). A recent analysis estimated global water sources receive up to 15,600 metric tons/yr (mt/yr) of TiO_2 ENMs and 3,700 mt/yr of ZnO ENMs (Keller *et al.*, 2013). Previous research, while limited, suggests that the increasing presence of ENMs in source waters has significant consequences for the formation of DBPs in disinfection and wastewater treatment systems (Dobrovic, 2012; Tugulea, 2014; Sharma, 2017; Yuan, 2013). For instance, a study by Metch *et al.* (2015) examined the impact of NPs on the formation of chloroform during chlorination of wastewater treatment plant (WWTP) effluent both with and without UV irradiation. The study found that certain NPs (i.e. AgNPs) greatly enhanced THM formation under a UV and free chlorine disinfection regime at all concentrations examined. There is a need, then, to assess the impact of NPs on DBP formation and toxicity during chlorination under environmentally relevant conditions (pH, light).

1.3 References

Barcelo, D., Postigo, C., Richardson, S., & Barceló, D. 2017. Formation of iodo-trihalomethanes, iodo-haloacetic acids, and haloacetaldehydes during chlorination and chloramination of iodine containing waters in laboratory controlled reactions. *J. Environ. Sci.* 58, 127-134.

Bermudez, E., Mangum, J.B., Wong, B.A., Asgharian, B., Hext, P.M., Warheit, D.B., et al. 2004. Pulmonary responses of mice, rats, and hamsters to subchronic inhalation of ultrafine titanium dioxide particles. *Toxicol. Sci.* 77, 347–357.

Bond, T., Mokhtar, N.H., Bonnisseau, T., Templeton, M.R. 2014. Disinfection by-product formation from the chlorination and chloramination of amines. *J. Hazard. Mater.* 278, 288-296.

Chen, B., & Westerhoff, P. 2010. Predicting disinfection by-product formation potential in water. *Water Research.* 44(13), 3755-3762.

Chu, W., Gao, N., Deng, Y., Krasner, S. 2010. Precursors of dichloroacetamide, an emerging nitrogenous dbp formed during chlorination or chloramination. *Environ. Sci. Technol.* 44, 3908.

Chu, W.H.; Gao, N.Y.; Deng, Y. 2010. Formation of haloacetamides during chlorination of dissolved organic nitrogen aspartic acid. *J. Hazard. Mater.* 173, 82.

Chueh, P. J., Liang, R., Lee, Y., Zeng, Z., Chuang, S. 2014. Differential cytotoxic effects of gold nanoparticles in different mammalian cell lines. *J. Hazard. Mater.* 264, 303-312.

Das, S., Kumar, A., Seth, R., Tokar, E., Kadiiska, M., Waalkes, M., Mason, R., Chaterjee, S. 2013. Proinflammatory adipokine leptin mediates disinfection byproduct bromodichloromethaneinduced early steatohepatic injury in obesity. *Toxicol. Appl. Pharmacol.* 269:297–306.

Diehl, A.C., Speitel, G., Symons, J.M., Krasner, S.W., Hwang, S.J., Barrett, S.E. 2000. DBP formation during chloramination. *American Water Works Assoc. J.*, 92(6), 76.

Ding, S., Deng, Y., Bond, T., Fang, C., Cao, Z., Chu, W. 2019. Disinfection byproduct formation during drinking water treatment and distribution: A review of unintended effects of engineering agents and materials. *Water Research*. 160:313-329.

Mahmoud, A., Ezgi, Ö., Merve, A., Özhan, G. 2016. In vitro toxicological assessment of magnesium oxide nanoparticle exposure in several mammalian cell types. *Int. J. Toxicol.* 35(4):429-437.

Faustino-Rocha, A. I., Rodrigues, D., da Costa, R. G., Diniz, C., Aragão, S., Talhada, D., Botelho, M., Colaço, A., Pires, M. J., Peixoto, F., Oliveira, P. A. 2016, Trihalomethanes in liver pathology: Mitochondrial dysfunction and oxidative stress in the mouse. *Environ. Toxicol.*, 31: 1009-1016.

Fotakis, G. & Timbrell, J. 2006. In vitro cytotoxicity assays: Comparison of LDH, neutral red, MTT and protein assay in hepatoma cell lines following exposure to cadmium chloride. *Tox. Letters.* 160(2), 171-177.

Golea, D.M., Upton, A., Jarvis, P., Moore, G., Sutherland, S., et al. 2017. THM and HAA formation from NOM in raw and treated surface waters. *Water Research.* 112, 226-235.

Goslan, E.H., Krasner, S.W., Bower, M., Rocks, S.A., Holmes, P., et al. 2009. A comparison of disinfection by-products found in chlorinated and chloraminated drinking waters in Scotland. *Water Res.* 43, 4698–4706

Hext, P., Tomenson, J., Thompson, P. 2005. Titanium Dioxide: Inhalation Toxicology and Epidemiology, *Annals Occu. Hyg.*, 49(6), 461–472.

Hong, H.C., Huang, F.Q., Wang, F.Y., Ding, L.X., Lin, H.J., et al. 2013. Properties of sediment NOM collected from a drinking water reservoir in south china, and its association with THMs and HAAs formation. *J. Hydrology.* 476, 274-279.

Hua, G., & Reckhow, D. 2007. Comparison of disinfection byproduct formation from chlorine and alternative disinfectants. *Water Res.* (Oxford), 41(8), 1667-1678.

Hung, Y., Waters, B. W., Yemmireddy, V. K., & Huang, C. 2017. pH effect on the formation of THM and HAA disinfection byproducts and potential control strategies for food processing. *J. Integ. Agri.* 16(12), 2095-3119.

Hunter, E.S., Pressman, J., Richardson, S., Speth, T., Miltner, R., et al. 2010. Concentration, chlorination, and chemical analysis of drinking water for disinfection byproduct mixtures health effects research: U.S. EPA's four lab study. *Environ. Sci. Tech.*, 44(19), 7184-7192.

Jiang, J. 2014. Advances in the development and application of ferrate(VI) for water and wastewater treatment. *J. Chem. Tech. Biotech.* 89(2), 165-177.

Juretic, H., Vrcek, I., Avdicevic, M., Dobrovic, S., Nemet, I., et al. 2012. Genotoxicity and effects of nanosilver contamination in drinking water disinfection. *Water Sci. Tech.*, 12(6), 829-836.

Konsoula, R., & Barile, F. A. 2005. Correlation of in vitro cytotoxicity with paracellular permeability in Caco-2 cells. *Toxicol. In Vitro.*, 19, 675−684.

Krasner, S. 2006. Occurrence of a new generation of disinfection byproducts. *Environ. Sci. & Tech.*, 40(23), 7175-85.

Liu, Y., Duan, J., Li, W., Lai, Q., Saint, C.P., et al. 2015. Determination of volatile disinfection byproducts in water by gas chromatography-triple quadrupole mass spectrometry. *Anal. Lett.* 48, 188–203.

Mitch, W., Sharp, J., Trussell, R., Valentine, R., Alvarez-Cohen, L., et al. 2003. Nitrosodimethylamine as a drinking water contaminant: a review. *Environ. Eng. Sci.* 20(5), 389-404.

Muellner, M., Wagner, E., McCalla, K., Richardson, S., Woo, Y., et al. 2007. Haloacetonitriles vs. regulated haloacetic acids: Are nitrogen-containing DBPs more toxic? *Environ. Sci. Tech.*, 41(2), 645-651.

Narotsky, M.G., Klinefelter, G.R., Goldman, J.M., DeAngelo, A.B., Best, D.S., et al. 2015. Reproductive toxicity of a mixture of regulated drinking-water disinfection by-products in a multigenerational rat bioassay. *Environ. Health Perspect.*, 123(6), 564-570.

Parvez, S., Rice, G., Teuschler, L., Simmons, J., Speth, T., et al. 2017. Method to assess component contribution to toxicity of complex mixtures: Assessment of puberty acquisition in rats exposed to disinfection byproducts. *J. Environ. Sci.*, 58, 311-321.

Plewa, M.J., Muellner, M.G., Richardson, S.D., Fasano, F., Buettner, K. M., et al. 2008. Occurrence, synthesis, and mammalian cell cytotoxicity and genotoxicity of haloacetamides: An emerging class of nitrogenous drinking water disinfection byproducts. *Environ Sci Technol.* 42(3):955-961.

Plewa, M.J. 2004. Chemical and biological characterization of newly discovered iodoacid drinking water disinfection byproducts. *Environ. Sci. Technol*. 38 (18), 4713-4722.

Plewa, M., Simmons, J., Richardson, S., Wagner, E. 2010. Mammalian cell cytotoxicity and genotoxicity of the haloacetic acids, a major class of drinking water disinfection by-products. *Environ. Mol. Muta.*, 51(8-9), 871-878.

Sedlak, D., & von Gunten, U. (2011). The chlorine dilemma. *Science.* 331(6013), 42-43.

Richardson, S.D., DeMarini, D.M., Kogevinas, M., Fernandez, P., Marco, E., et al. (2010). What's in the Pool? A Comprehensive Identification of Disinfection By-products and Assessment of Mutagenicity of Chlorinated and Brominated Swimming Pool Water. *Environ. Health Perspect*. 118, 1523.

Richardson, S., & Kimura, S. 2015. Water analysis: Emerging contaminants and current issues. *Analytical Chem.* 90(1), 546-582.

Richardson, S., Fasano, F., Ellington, J.J., Crumley, F.G., Buettner, K., et al. 2008. Occurrence and Mammalian Cell Toxicity of Iodinated Disinfection Byproducts in Drinking Water. Environ. *Sci. Tech.*, 42(22), 8330-8338.

Richardson, S., Postigo, C. 2018. Liquid chromatography−mass spectrometry of emerging disinfection by-products. In Advances in the Use of Liquid Chromatography Mass Spectrometry (LC-MS). *Instrumentation Developments and Applications*. Elsevier: Amsterdam, pp 267.

Richardson, S., Richardson, A., Thruston, S., Krasner, H., Weinberg, R., et al. 2008. Integrated disinfection by-products mixtures research: Comprehensive

characterization of water concentrates prepared from chlorinated and ozonated/postchlorinated drinking water. *Toxicol. Environ. Health*, Pt. A 71, 1165.

Richardson, S.D., Thruston, A.D., Collette, T.W., Patterson, K.S., Lykins, B.W., Ireland, J.C. 1996. Identification of TiO2/UV disinfection byproducts in drinking water. *Environ Sci Technol.* 30(11):3327-3334.

Rook, J. 1974. Formation of haloforms during chlorination of natural waters. *Water Treat. Exam.* 23, 234-243.

Shah, A., & Mitch, W. 2012. Halonitroalkanes, halonitriles, haloamides, and n-nitrosamines: A critical review of nitrogenous disinfection byproduct formation pathways. *Environ. Sci. Tech.,* 46(1), 119-131.

Sharma, V. 2013. Ferrate(VI) and ferrate(V) oxidation of organic compounds: Kinetics and mechanism. *Coordination Chem. Reviews,* 257(2), 495-510.

Sharma, V., Yang, X., Cizmas, L., McDonald, T. J., et al. 2017. Impact of metal ions, metal oxides, and nanoparticles on the formation of disinfection byproducts during chlorination. *Chem. Eng. J.*, 317, 777-792.

Sharma, V., Zboril, R., & Varma, R. 2015. Ferrates: Greener oxidants with multimodal action in water treatment technologies. *Acc. Chem. Research*, 48(2), 182-191.

Stalter, D., O'Malley, E.,Von Gunten, U., & Escher, B. 2016. Fingerprinting the reactive toxicity pathways of 50 drinking water disinfection by-products. *Water Res.* 91, 19–30.

Villanueva, C., Cantor, K., Grimalt, J., Castano-Vinyals, G., Malats, N., et al. 2006. Assessment of lifetime exposure to trihalomethanes through different routes. *Occu. Environ. Med.* 63, 273–277.

Verdugo, E.M., Krause, C., Genskow, K., Han, Y., Baltrusaitis, J., et al. 2014. N-functionalized carbon nanotubes as a source and precursor of N-nitrosodimethylamine: Implications for environmental fate, transport, and toxicity. *Environ Sci Technol.* 48(16):9279-9287.

Verdugo, E.M., Nelson, K.J., Bako, C.M., Valentine, R.L., Cwiertny, D.M. 2016. Formation of trihalomethanes and haloacetic acids during chlorination of functionalized carbon nanotubes. *Environ Sci: Nano.* 3(6):1327-1339.

Warner, N., Christie, C., Jackson, R., Vengosh, A. 2013. Impacts of shale gas wastewater disposal on water quality in western Pennsylvania. *Environ. Sci. Technol.* 47, 11849-11857.

Yang, M., Zhang, X. 2016. Current trends in the analysis and identification of emerging disinfection byproducts. *Trends Environ. Anal. Chem.* 10, 24−34.

Zhai, H., Zhang, X., Zhu, X., Liu, J., & Ji, M. 2014. Formation of Brominated Disinfection Byproducts during Chloramination of Drinking Water: New Polar Species and Overall Kinetics. *Environ. Sci. Tech.*, 48(5), 2579-2588.

Zhang, H., Wang, X., Wang, M., Li, L., et al. 2015. Mammalian cells exhibit a range of sensitivities to silver nanoparticles that are partially explicable by variations in antioxidant defense and metallothionein expression. *Small* (Weinheim an Der Bergstrasse, Germany), 11(31), 3797-3805.

2. A MULTI-STEP APPROACH TO ASSESSING AND COMPARING DISINFECTION BYPRODUCT FORMATION AND CYTOTOXICITY FOLLOWING CHLORINATION OR FERRATE(VI) DISINFECTION

2.1. Introduction

Establishing new options for disinfection will play a critical role in the future development and stability of potable water resources. Yet, any novel disinfectant – no matter how promising – must be sufficiently measured against conventional chlorine-based disinfectants to fully assess its impact on prevailing environmental and water quality health issues. The generation of disinfectant byproducts (DBPs) is one risk associated with the use of conventional chlorine-based disinfectants. DBPs are a hazardous class of compounds associated with cancers of the bladder, colon, and kidneys as well as adverse pregnancy outcomes (Richardson, 2015; Villanueva, 2006). They stem from the oxidative interactions of chlorinated disinfectants with natural organic matter (NOM) and halides (e.g. bromide and iodide) present in raw waters. To circumvent the host of potential health risks associated with chronic DBP exposure, there is growing interest in the compound ferrate(VI) [$\mathbf{Fe^{VI}O_4^{2-}}$; Fe(VI)] as a potential replacement for conventional chlorine-based disinfectants. It is characterized as a strong oxidant and hydroxylating agent, capable of inactivating various microorganisms (e.g. *E. coli*, *Bacillus subtilis*, total coliforms, and viruses), detoxifying toxins (e.g. microcystins, heavy metals), degrading organic and inorganic impurities, and removing colloidal/particulate materials (Jiang, 2014; Sharma, 2013). Fe(VI), however, remains at

the initial stages of development as an alternative disinfectant, and its potential interactions with DBP precursors (including the formation of complex DBP mixtures) are largely unknown. In order to advance towards acceptance as an improved disinfection method, there is a need to conduct a full assessment of DBP formation and the cytotoxicity of potential complex DBP mixtures following ferrate treatment.

Previous research surrounding the influence of Fe(VI) on DBP formation/toxicity has focused heavily on identifying and quantifying individual DBPs and DBP species resulting from Fe(VI) interactions with NOM. A study by Sharma (2010), for example, measured ferrate reactivity with the Br^- ion, and found that the reactive species of bromine necessary to produce Br-DBPs would not be produced during Fe(VI) treatment. Jiang *et al.* (2016) demonstrated that, at typical doses, direct ferrate oxidation of raw water reduced the production of certain DBP species [30% for THMs, 40% for trihaloacetic acids (THAAs), 10% for dihaloacetic acids (DHAAs), 30% for dihaloacetonitriles (DHANs), and 5% for haloketones (HKs)]. Another study by Gan *et al.* (2015) showed that pre-oxidation with Fe(VI), followed by chlorination, suppressed the formation of THMs, chloral hydrate (CH), and HAN, but had no effect on trichloronitromethane (TCNM) concentrations compared to treatment with chlorination alone. As such, the data available on Fe(VI)'s influence on the generation and overall toxicity of complex DBP mixtures compared to chlorination remains limited.

The overall goal of this study was to compare DBP formation and cytotoxicity following disinfection of synthetic drinking water with either chlorine or ferrate(VI). To this end, a combination of chemical analyses and biological assays were employed using

Chinese hamster ovary cells [CHO-K1 (ATCC CRL-9618)] and human colorectal adenocarcinoma cells [Caco-2 (ATCC® HTB-37™). CHO-K1 cells are a well-established cell line, widely used as the gold-standard for DBP toxicity assays on mammalian cells (Poul, 2004; Wagner, 2017; Wang, 2014). The CaCo-2 cell line was chosen because it is often employed in the same capacity as *in vitro* rodent cytotoxicity assays, but with a focus on human-based DBP exposures [Hebels, 2009; Konsoula, 2005; Neale, 2012]. The CaCo-2 cell line is relevant to the colorectal region which would be impacted by contaminants in drinking water, such as DBPs (Prochazka, 2015). Additionally, CaCo-2 cells retain certain phase I (i.e. Cytochrome P450 CYP1A1, CYP1A2, CYP2B and CYP2E1) and phase II enzymes (i.e. glutathione-S-transferases, sulfotransferases, N-acteyltransferases, and glucuranosyltransferases) which mimic *in vivo* metabolic responses toward toxic and carcinogenic compounds.

The objectives of this study were to disinfect simulated drinking water samples with either ferrate(VI) [(FeVI), (FeO42-)] or chlorine, then 1) chemically analyze the formation of nine DBPs of interest; 2) determine the overall cytotoxicity of the DBPs in these samples; and 3) compare the chemical and biological data for the ferrate(VI)-treated and chlorine-treated samples to assess differences in DBP formation and cytotoxicity. It was hypothesized Fe(VI)-treated waters would be less cytotoxic than chlorine-treated waters.

2.2. Materials & Methods

2.2.1. Chemicals & Reagents

General reagents were certified ACS reagent grade and were purchased from Fisher Scientific (Itasca, IL) and Sigma-Aldrich (St. Louis, MO) (See Appendix B, Table 1 for details). Potassium iodide (KI) and sodium bromide (NaBr) were purchased from Fisher Scientific (Itasca, IL) and Sigma-Aldrich (St. Louis, MO). Suwanee River natural organic matter (NOM) was purchased from the International Humic Substances Society (IHSS; St. Paul, MN). F-12K media, fetal bovine serum (FBS), EDTA-trypsin, and penicillin/streptomycin mixtures were purchased from the American Type Culture Collection (ATCC; Manassas, VA). Oasis HLB cartridges (6 cc, 150 mg, 30 μm particle size) for solid-phase extraction (SPE) were purchased from Waters (Milford, MA). All solvents [acetonitrile, n-hexane, methanol, dimethyl sulfoxide (DMSO)] were of highest purity and were purchased from Fisher Scientific (Itasca, IL), Sigma-Aldrich (St. Louis, MO), or VWR International (Radnor, PA). Chemical properties, purity, and CAS numbers of all compounds are provided in Appendix B (Table 1).

2.2.2. Preparation of Water Samples

The synthetic water was prepared based on the average concentration of constituents found in a typical sample of surface freshwater from in the contiguous United States (Amy, 1993). All synthetic water used in this study had the same composition and contained ultra-pure Milli-Q water, Suwannee River NOM, potassium iodide (KI), sodium bromide (NaBr), and phosphate buffer. After adjustment to pH 7.00, filtration, and a 24 hour stir period prior to disinfection, samples were disinfected with

chlorine, Fe(VI), or not disinfected (control sample). Following this treatment, all samples including the control were allowed to stir for an additional 48 hours and then split into 6 aliquots per treatment. A small portion of each sample was removed for chemical analysis.

The samples were each filtered through a dry 0.45 µm Durapore Membrane Filter (HVLP04700; SIGMA; St. Louis, MO) to remove any impurities. Next, the samples where extracted using solid phase extraction (SPE) with Oasis HLB cartridges (186000117; Waters; Milford, MA). The SPE cartridges were conditioned prior to the beginning of the extraction process by the addition of methanol (MeOH), followed by Milli-Q water. The samples were then extracted using a flow rate through the SPE cartridge of approximately 5 mL/minute. A maximum of 2L of samples was extracted with each cartridge. The cartridges containing the sample extracts were then inserted into a vacuum manifold above collection vials and the samples were eluted with methanol and a hexane:acetone mixture.

2.2.3. Concentration of the Extract

After extraction, the samples were dehydrated with anhydrous sodium sulfate. The column and wool used for this procedure were pre-washed with MeOH and a hexane:acetone solvent mixture. The samples were then each poured through a column and allowed to drain into a collection vial. A total of 10 µL of DMSO was added to each of the vials to protect the sample against complete evaporation. A TurboVap Evaporator System (Biotage; Charlotte, NC) was used for solvent reduction and solvent exchange. The samples were placed into the TurboVap and the volume was allowed to reduce for

approximately 20-30 minutes. Before reaching 5 mL, the edges of the vials were quantitatively rinsed with MeOH and hexane:acetone and allowed to reduce back down to approximately 5 mL. Kuderna-Danish concentrator tubes were used to further concentrate the samples. Care was taken to prevent the samples from reaching dryness during the concentration process. Once the samples reached just below their final volume, they were immediately extracted from the water bath and brought up with DMSO. The final product was a DBP/DMSO mixture at a volume that was 1/8000th of the initial water sample volume [i.e. an 8000x concentration factor (CF) was used].

2.2.4. Chemical Analyses

A portion of each water sample was shipped to Alexin Analytical Laboratories (Tigard, OR), a National Environmental Laboratory Accreditation Program (NELAP) approved lab which met all TNI Standards for DBP (TTHM/HAA5) analysis by gas chromatography/mass spectrometry (GC/MS) determination. All analyses were conducted according to EPA Methods 524.2 (TTHM; Revision 4.1) and 552.1 (HAA5; Revision 1.0) (see sections 9 & 10 of each method for quality control and calibration measures). Immediately after treatment with ferrate or chlorine (or no treatment for the control), samples were aliquoted out for chemical analysis. To prevent the loss of THMs, the aliquots for THM analyses were collected as follows. Four 40 mL vials with a septum (containing 3 mg of sodium thiosulfate, provided by Alexin Labs) were filled according to instructions provided by Alexin Labs. Just before aliquoting out the sample, the rubber stopper in the Erlenmeyer flask containing the sample was removed and quickly replaced with parafilm. Using a 25 mL pipette and serological pipettor, the

parafilm was peeled back just enough to place the pipette tip into the liquid and retrieve the required amount. Between pipettes, the parafilm was immediately replaced and the used pipette was exchanged for a fresh one. The pipette tip was placed into the bottom of a vial and the sample was gently pipetted out, while making sure the tip of the pipette tip remained below the water level. This process was repeated until the vial was full, with no remaining headspace once capped. Once all of the vials were filled, they were labeled with a sample ID, date and initials. Upon collection, the vials were placed upside down in a refrigerator immediately to cool. For HAA analysis, the same process was completed except for a total of two 125 ml amber flasks (containing crystalline ammonium chloride; provided by Alexin Labs) per sample. Unlike the THM vials, the HAA flasks were left with headspace according to the instructions of Alexin Labs. After collection and a 24-hour storage period, the samples were placed inside a small cooler, packed with blue ice and packaging materials, and then shipped to Alexin Labs for chemical analysis.

2.2.5. Cell Lines

2.2.5.1. Chinese Hamster Ovary Cells

The Chinese hamster ovary (CHO) cell line CHO-K1 (ATCC® CRL-9618™) was used to assess cytotoxicity. The CHO-K1 cells were maintained in complete growth media, consisting of F-12K Medium, 5% FBS, and 1% antibiotics (100 U/mL sodium penicillin G, 100 μg/mL streptomycin sulfate) at 37 °C in a humidified atmosphere of 5% CO2.

2.2.5.2. Human Colorectal Adenocarcinoma Cells

The human colorectal adenocarcinoma (CaCo) cell line CaCo-2 (ATCC® HTB-37™) was used to assess cytotoxicity. The CaCo-2 cells were maintained in complete growth media, consisting of Eagle's Minimum Essential Medium (EMEM) (ATCC® 30-2003™), 20% FBS, and 1% antibiotics (100 U/mL sodium penicillin G, 100 μg/mL streptomycin sulfate) at 37 °C in a humidified atmosphere of 5% CO2.

2.2.6. Chronic Cell Cytotoxicity Assays

The 96-well microplate assay for chronic cytotoxicity in mammalian cells measures the reduction in cell density as a function of the sample extract concentration over a period of 72 hours (~3 cell cycles). Chinese hamster ovary (CHO-K1) and human colon cancer (CaCo-2) cell lines were plated in 96-well flat-bottomed microplates in complete growth media. The cells were then treated with a 10x serial dilution (from $1.00x10^{-3}$ to $1.00x10^{-6}$%) of the sample extracts to produce a range of relative enrichment factors (REF) (from $8.0x10^{-3}$x to 8.0x) [CF × Dilution Factor (DF)]. The cells were then incubated for 72 hours at 37°C and 5% CO_2. For each sample extract concentration, 8 replicates were fixed with methanol and stained with a 1% crystal violet solution. Each microplate's absorbance was then analyzed at 570 nm with a plate reader. The individual assays were repeated 3 times and the absorbance values from each column were averaged to create a mean absorbance value for the treatment group. A mean value of the blank-corrected absorbance values of the negative control columns (cells with media only) was subtracted from the absorbance of each treatment group. The corrected absorbance for each treatment group well was then converted into a percentage

of the mean absorbance obtained from solvent control column in order to provide the graphs more consistency.

2.2.7. Statistical Analyses

For the chronic cytotoxicity assays, two-way analysis of variance (ANOVA) tests with interacting terms were conducted to determine if a sample induced a statistically significant change in cell density in both cell lines as compared to a control at the corresponding dilution level. If a significant F value ($P \leq 0.05$) was obtained, a pair-wise multiple comparison procedure (Bonferroni t-test) was performed. The power of the test statistic ($1-\beta$) was maintained as ≥ 0.8 at $\alpha = 0.05$.

2.3. Results

2.3.1. Chemical Analysis

The effect of disinfectants on the production of regulated THMs and HAAs in synthetic drinking water samples was investigated (Fig. 2.1). Out of the three disinfectants employed, only the chlorinated samples had detectable levels of THMs. Across the three sets of chlorinated samples, the mean THM amounts were 2.53×10^{-2} mg/L of chloroform, 2.30×10^{-3} mg/L of BDCM, and 2.76×10^{-2} mg/L of TTHM. Non-disinfected samples and samples treated with Fe(VI) contained no THMs according to GC/MS analysis. Only the chlorinated samples contained detectable levels of HAAs (Fig. 2.2). The mean HAA amounts for the three sets of chlorinated samples were 3.16×10^{-3} mg/L of CAA, 2.09×10^{-2} mg/L of DCAA, 9.56×10^{-3} mg/L of TCAA, and 3.36×10^{-2} mg/L of HAA5. Non-disinfected samples and samples treated with ferrate did not contain any HAAs according to GC/MS analysis.

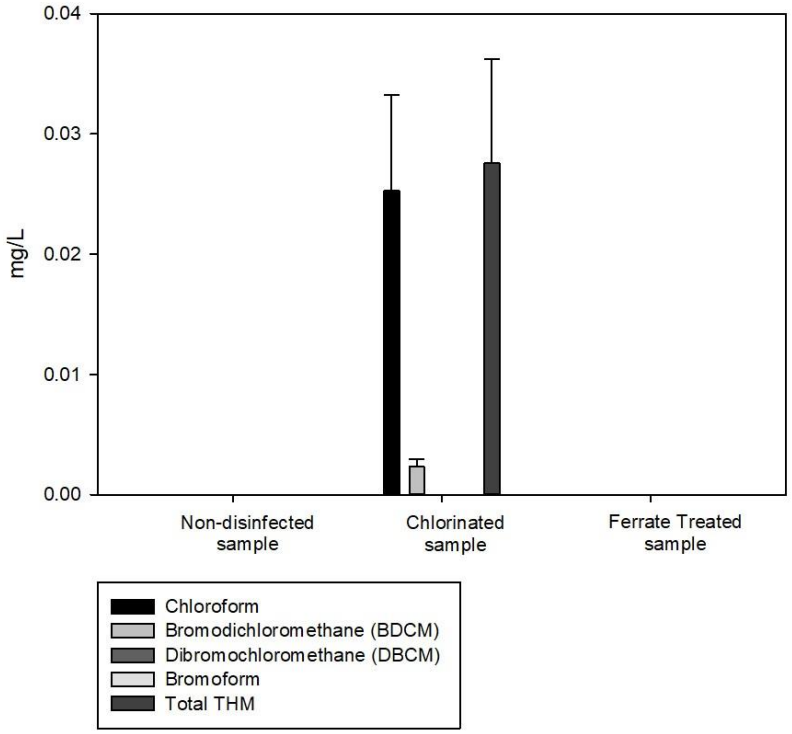

Figure 2.1 Effect of disinfectants on trihalomethane concentrations: chemical analysis results showing the occurrence of regulated trihalomethanes (mg/L) in synthetic drinking water samples treated under different disinfectants (Chlorine or Ferrate). Disinfection byproduct (DBP) analysis of HAAs was accomplished via gas chromatography/mass spectrometry (GC/MS) determination. The minimum reporting limit (MRL) was 1-2 ng/L. All HAA analyses were conducted according to EPA Method 552.1.

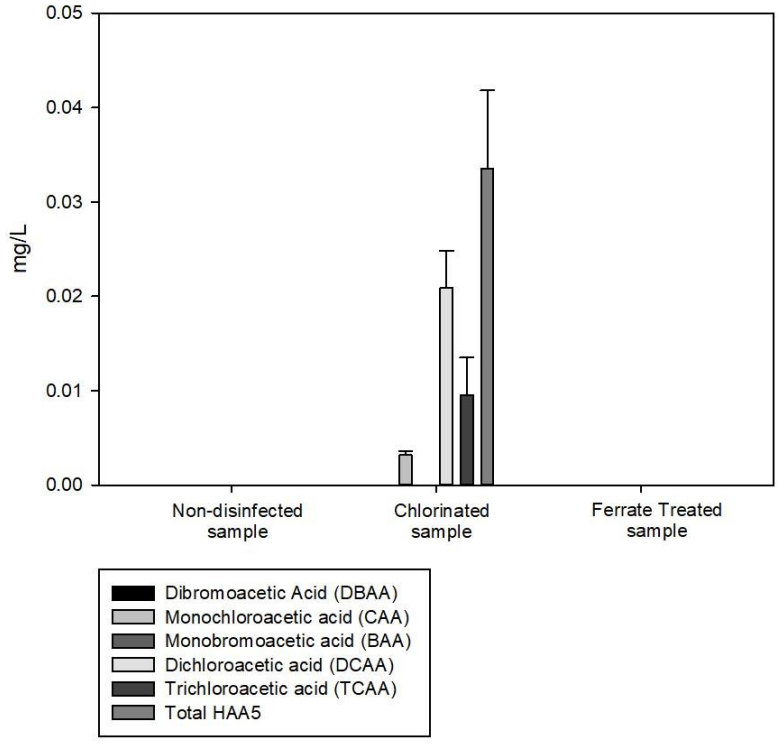

Figure 2.2 Effect of disinfectants on haloacetic acid concentrations: chemical analysis results showing the occurrence of regulated haloacetic acids (HAAs) (mg/L) in synthetic drinking water samples treated under different disinfectants (Chlorine or Ferrate). Disinfection byproduct (DBP) analysis of HAAs was accomplished via gas chromatography/mass spectrometry (GC/MS) determination. The minimum reporting limit (MRL) was 1-2 ng/L. All HAA analyses were conducted according to EPA Method 552.1.

It was expected that no DBPs would be formed in samples disinfected with ferrate(VI) since DBPs form as a result of reactions of disinfectants (e.g. chlorine or chloramine) with NOM moieties and/or halides already present in source waters. Ferrate(VI), unlike conventional chlorine-based chemical disinfectants, does not interact with bromide ions and is rapidly reduced to non-toxic iron(III) during oxidation

reactions which aids in the flocculation and precipitation of source water constituents (Jiang J. & Wang S., 2003; Jiang J., 2014; Sharma, 2013; Sharma *et al.*, 2015). These combined processes limit direct oxidative interactions of Fe(VI) with NOM and an important DBP-producing halide. As such, Fe(VI) is not expected to produce any of the regulated DBPs commonly observed under other chlorine-based disinfectants.

2.3.2. Chronic Cell Cytotoxicity Assays

2.3.2.1. CHO-K1 Cellular Assay

The chronic cytotoxicity of these synthetic drinking water extracts was investigated using CHO-K1 cells. Fig. A.1 (included in Appendix A) shows the differences in mean recorded density of CHO-K1 cell cultures after a 72hr exposure period to different sample types [i.e. control, chlorinated, Fe(VI)] over a relative enrichment factor (REF) range of $8.0x10^{-3}x$ to 8.0x. While some minor variations were recorded, statistical analysis indicated that the difference in values when factoring for sample type, dilution level, and interactions between the two factors were all non-significant ($P>0.05$). In effect, there was no significant difference in cytotoxicity levels between the different treatments or their various sample concentrations.

2.3.2.2. CaCo-2 Cellular Assay

The cytotoxicity of these samples produced under different disinfectant regimens in CaCo-2 cells was also investigated. Fig. A.2 (included in Appendix A) shows the differences in mean recorded density of CaCo-2 cell cultures after a 72hr exposure period to different sample types (i.e. control, chlorinated, ferrate) over a REF range of $8.0x10^{-3}x$ to 8.0x. Statistical analysis indicated that the difference in cytotoxicity levels

when factoring for sample type, alone, was significant ($P \geq 0.05$). However, factoring for dilution level and interactions between sample type and dilution level showed no statistical significance ($P \leq 0.05$). Essentially, there was no significant difference in cytotoxicity levels between the different treatments or their various sample concentrations once their dilution levels were accounted for.

Significant differences in cytotoxicity were not seen in either CHO-K1 or CaCo-2 assays. Recorded DBP levels in the water samples were barely above detection level, as indicated in the chemical analysis results. Due to the low concentrations of water constituents and high purity of the water, it is likely that the levels for both detected and undetected DBPs were too low to produce any significant cytotoxic effects in the cell cultures.

2.4. Conclusions

Results comparing the effects of a novel disinfectant with chlorination on DBP formation suggest that, under the conditions of this study, Fe(VI) produced none of the DBPs detected during conventional chlorination. Most regulated DBPs are either chlorinated or brominated species. Ferrate(VI) contains no chlorine as part of its chemical structure so it cannot contribute to any DBP that is formed. In addition, Fe(VI) does not interact with bromide ions and is rapidly reduced to non-toxic iron(III) during disinfection (Jiang J. & Wang S., 2003; Jiang J., 2014; Sharma, 2013; Sharma *et al.*, 2015). As such, Fe(VI) does not produce any of the DBPs (all chlorinated or brominated species) analyzed in this study. The data do not suggest that Fe(VI) cannot produce other

unregulated DBPs, only that it prevents the production of most regulated varieties under the conditions of this study.

Results from the CHO-K1 and CaCo-2 cytotoxicity assays, however, did not show a significant difference in cytotoxicity between the various treatments. When compared with chlorinated and control samples, Fe(VI) produced no significant decrease in cytotoxicity despite producing fewer measured DBPs. These results were likely the product of low-level DBP formation in the initial synthetic water samples. Variability in DBP production is a difficult issue to address. This is particularly true when looking at complex DBP mixtures as opposed to individual DBP species. Concentrations of DBPs vary temporally and geographically according to the physiochemical properties of the source water (Grellier, 2015). In an attempt to overcome limitations in reproducibility inherit with using local source water, this study created synthetic water samples dosed with national NOM and halide averages. While this approach allowed for the generation of more reproducible source waters, the relative purity of the water and its constituents (compounded by a series of filtrations) may have limited DBP formation rates as compared to a natural source water. As evidenced by the chemical analyses, the average amounts of THMs and HAAs contained in these samples did not exceed a total of 33.6 ng/L, barely above the method reporting limit (MRL) of the GC/MS used for this study (1 to 2 ng/L). This, in turn, may have contributed to the limited cytotoxicity levels seen in the different sample concentrations. Even so, there is a possibility (however limited) that Fe(VI) may have produced other unregulated DBPs that negated its advantages for DBP production compared to chlorination. Overall, this study emphasizes the need for

additional research on DBP formation by Fe(VI), including testing water extracts that are more concentrated, and using additional types of toxicity assays.

2.5. References

Amy, G., Siddiqui, M., Zhai, W., DeBroux, J., Odem, W. 1993. Nation-wide survey of bromide ion concentrations in drinking water sources. *American Water Works Association Proceedings*, 1993 Annual Conference, San Antonio, TX.

Grellier, J., Rushton, L., Briggs, D.J., Nieuwenhuijsen, M.J. 2015. Assessing the human health impacts of exposure to disinfection by-products – A critical review of concepts and methods. *Environ. Inter.* 78:61-81.

Hebels, Dennie G.A.J., Jennen, D.G.J., Kleinjans, J.C.S., & de Kok. 2009. Molecular signatures of N-nitroso compounds in Caco-2 cells: Implications for colon carcinogenesis. *Tox. Sci.*, 108(2), 290-300.

Jiang, J. 2014. Advances in the development and application of ferrate(VI) for water and wastewater treatment. *J. Chem. Tech. Biotech.* 89(2):165-177.

Jiang, J., Wang, S. 2003. Enhanced coagulation with potassium ferrate(VI) for removing humic substances. *Environ. Eng. Sci.* 20(6):627-633.

Liu, Y., Bodmer, W. 2006. Analysis of P53 mutations and their expression in 56 colorectal cancer cell lines. *Proc. Natl. Acad. Sci USA*. 103(4):976-981.

Neale, P., Antony, A., Bartkow, M., Farré, M., Heitz, A., Kristiana, I., Escher, B. 2012. Bioanalytical assessment of the formation of disinfection byproducts in a drinking water treatment plant. *Environ. Sci. Tech.*, 46(18).

Osburn, W.O., Kensler, T.W. 2008. Nrf2 signaling: An adaptive response pathway for protection against environmental toxic insults. *Mut. Res./Rev. Mut. Res*. 659(1):31-39.

Poul, J. M., Huet, S., Godard, T., & Sanders, P. 2004. Lack of genotoxicity of potassium iodate in the alkaline comet assay and in the cytokinesis-block micronucleus test. Comparison to potassium bromate. *Food Chem. Tox.*, 42(2), 203-209.

Prochazka, E., Escher, B.I., Plewa, M.J., Leusch, F.D.L. 2015. In vitro cytotoxicity and adaptive stress responses to selected haloacetic acid and halobenzoquinone water disinfection byproducts. *Chem. Res. Toxicol.* 28(10).

Sharma, V. (2010). Oxidation of inorganic compounds by ferrate(VI) and ferrate(V): one-electron and two-electron transfer steps. *Environ. Sci. Technol.* 45, 5148–5152.

Sharma, V. (2013). Ferrate(VI) and ferrate(V) oxidation of organic compounds: Kinetics and mechanism. *Coordination Chem. Reviews*, 257(2), 495-510.

Sharma, V., Zboril, R., & Varma, R. 2015. Ferrates: Greener oxidants with multimodal action in water treatment technologies. *Acc. Chem. Research*, 48(2), 182-191.

Wagner, E., & Plewa, M. 2017. CHO cell cytotoxicity and genotoxicity analyses of disinfection by-products: An updated review. *J. Environ. Sci.*, 58, 64-76.

Wang, W., Qian, Y., Li, J., Moe, B., Huang, R., et al. 2014. Analytical and toxicity characterization of halo-hydroxyl-benzoquinones as stable halobenzoquinone disinfection byproducts in treated water. *Analytical Chem.*, 86(10), 4982-4988.

3. A MULTI-STEP APPROACH TO ASSESSING DISINFECTION BYPRODUCT FORMATION AND CYTOTOXICITY OF SYNTHETIC DRINKING WATERS DOSED WITH TITANIUM DIOXIDE (TiO_2) OR ZINC OXIDE (ZnO) NANOPARTICLES.

3.1. Introduction

Engineered nanomaterials (ENMs) are an emerging contaminant produced for an increasingly wide variety of applications (e.g. industrial, biomedical, and consumer products). Previous research suggests that the increasing presence of ENMs may have significant consequences for the formation of disinfection byproducts (DBPs) in disinfection systems (Dobrovic, 2012; Metch, 2015; Tugulea, 2014; Sharma, 2017; Yuan, 2013). Titanium dioxide (TiO_2) and zinc oxide (ZnO) nanoparticles (NPs) are among the highest volume produced of all nanomaterials and are used in a wide range of industrial, biomedical, and consumer product applications (e.g. textiles, paint pigments, medical equipment, sunscreens, printing ink, packaging materials, etc.) (Richardson and Ternes, 2014). The presence of TiO_2 and ZnO NPs in source waters may compound the issues of DBP production and toxicity during chlorination by creating a potential alternate route for DBP production (Dobrovic, 2012; Tugulea, 2014; Sharma, 2017; Yuan, 2013). Examining how the presence of microcontaminants like TiO_2 and ZnO might impact DBP formation and DBP toxicity in finished drinking water is critical toward assessing the potential public health risks and hazards associated with such interactions. The effects of emerging contaminants on the formation and toxicity of

DBPs following chlorination of drinking water is a pressing health concern. Previous studies have focused heavily on the impact of silver nanoparticles (Ag NPs) in producing individual DBPs, often with limited environmental relevance evident in their design (Dobrovic, 2012; Metch, 2015; Tugulea, 2014). For instance, Metch, *et al*. (2015) applied a 20 mg/L dosage of AgNPs to chlorinated and UV-treated waters which then demonstrated a significant increase in chloroform levels. The 20 mg/L dosage, however, is outside any naturally occurring level. There is a need, then, to assess the impact of other widespread NPs on the formation of complex DBP mixtures and the toxicity of these mixtures during chlorination under environmentally relevant conditions (dosage, pH, light).

The objectives of this study were to disinfect simulated drinking water samples dosed with NPs [TiO_2, ZnO, or none (control)] and exposed to UV light with chlorine, then 1) chemically analyze the formation of nine DBPs of interest; 2) determine the overall cytotoxicity of the DBPs in these samples; and 3) compare the chemical and biological data for the TiO_2-dosed, ZnO-dosed, and control samples to assess differences in DBP formation and cytotoxicity. It was hypothesized NP-dosed water samples would produce more DBPs and be more cytotoxic than the control samples.

3.2. Materials & Methods

3.2.1. Chemicals & Reagents

All reagents (certified ACS reagent grade) were purchased from Fisher Scientific (Itasca, IL) and Sigma-Aldrich (St. Louis, MO) (See Appendix B, Table 1 for additional details). Suwanee River natural organic matter (NOM) was purchased from the

International Humic Substances Society (IHSS; St. Paul, MN). TiO_2 nanoparticles, ZnO nanoparticles, potassium iodide (KI), and sodium bromide (NaBr) were all purchased from either Fisher Scientific (Itasca, IL) or Sigma-Aldrich (St. Louis, MO). Oasis HLB cartridges (6 cc, 150 mg, 30 μm particle size) were purchased from Waters (Milford, MA). Penicillin/streptomycin mixtures, F-12K media, fetal bovine serum (FBS), and EDTA-trypsin were purchased from the American Type Culture Collection (ATCC; Manassas, VA). All solvents [acetonitrile, n-hexane, methanol, dimethyl sulfoxide (DMOS)] were of highest purity and were purchased from Fisher Scientific (Itasca, IL), Sigma-Aldrich (St. Louis, MO), and VWR International (Radnor, PA). Chemical properties, purity, and CAS numbers of all compounds are available in Appendix B, Table 1.

3.2.2. Preparation of Nanoparticle Water Samples

Synthetic water mixtures were prepared according to the description in the previous chapter (Section 2.1.2). Synthetic water samples were generated consisting of ultra-pure Milli-Q water, NOM, KI, NaBr, and MES hydrate buffer. After pH adjustment to 7.0, filtration, and a 24 hour stir period, the samples were dosed with nanoparticles [TiO_2, ZnO, or no nanoparticles (control)], put in a dark area directly in front of a long-wave (365 nm) UV light, and allowed to stir for an additional 2-hour period. The samples were then disinfected with chlorine. Immediately after disinfection, a small portion of the water samples was removed for chemical analysis.

3.2.3. Concentration of the Extract

The remaining sample volumes were pre-concentrated by solid phase extraction (SPE) according to the procedure described in the previous chapter (Section 2.2.3.). After extraction, the samples underwent elution, dehydration, and concentration/solvent exchange as described in the previous chapter (Section 2.2.3). The final product was a DBP/DMSO mixture 1/8000th of the original combined sample volumes [8000x concentration factor (CF)].

3.2.4. Chemical Analyses

In accordance with the procedure described in the previous chapter (Section 2.2.4.), a portion of each water sample was collected, stored, and shipped to Alexin Analytical Laboratories (Tigard, OR), a NELAP accredited lab, for DBP (TTHM/HAA5) analysis by gas chromatography/mass spectrometry (GC/MS) determination. All analyses were conducted according to EPA Methods 524.2 (TTHM; revision 4.1) and 552.1 (HAA5; Revision 1.0) (See sections 9 & 10 of both methods for quality control and calibration procedures).

3.2.5. Cell Lines

3.2.5.1. Chinese Hamster Ovary Cells

The Chinese hamster ovary (CHO) cell line CHO-K1 (ATCC® CRL-9618™) was used to assess cytotoxicity and maintained according to the procedure described in the previous chapter (Section 2.2.5.1.). The CHO cells were maintained in complete growth media, consisting of F-12K Medium, 5% FBS, and 1% antibiotics (100 U/mL

sodium penicillin G, 100 μg/mL streptomycin sulfate) at 37 °C in a humidified atmosphere of 5% CO2.

3.2.5.2. Human Colon Adenocarcinoma Cells

The human colon adenocarcinoma cell line CaCo-2 (ATCC® HTB-37™) was also used to assess cytotoxicity. It was maintained according to the procedure described in the previous chapter (Section 2.2.5.2.). The CaCo cells were maintained in complete growth media, consisting of Eagle's Minimum Essential Medium (EMEM) (ATCC® 30-2003™), 20% FBS, and 1% antibiotics (100 U/mL sodium penicillin G, 100 μg/mL streptomycin sulfate) at 37 °C in a humidified atmosphere of 5% CO2.

3.2.6. Cytotoxic Bioassays

The 96-well microplate assay for chronic cytotoxicity in mammalian cells measures the reduction in cell density as a function of the DBP mixture concentration over a period of 72 h (~3 cell cycles). The detailed procedure is described in the previous chapter (Section 2.2.6). For each sample concentration, eight replicates were stained with 1% crystal violet solution and analyzed by microplate reader at an absorbance of 570nm. The individual assays were repeated three times and the absorbance values of each treatment column were averaged into a mean absorbance value. The mean absorbance value of the negative control column (cells with media only) was subtracted from the mean absorbance of each treatment column to produce a mean corrected absorbance value. The corrected absorbance for each treatment group was then converted into a percentage of the mean absorbance of the solvent control to provide the graphs with greater consistency.

3.2.7. Statistical Analyses

For the chronic cytotoxicity assays, two-way ANOVA tests with interaction terms were conducted following the same method described in the previous chapter (Section 2.2.7.) to determine if the NP-dosed samples induced a statistically significant change in cell density among cell lines as compared to the control samples of corresponding dilution level. If a significant F value ($P \leq 0.05$) was obtained, a pair-wise multiple comparison analysis was performed (Bonferroni t-test). The power of the test statistic ($1-\beta$) was maintained as ≥ 0.8 at $\alpha = 0.05$.

3.3. Results

3.3.1. Chemical Analysis

The effect of TiO_2 and ZnO nanoparticles on the production of regulated THMs and HAAs in synthetic water samples was investigated. Fig. A.3 (included in Appendix A) shows the average levels of THMs that each synthetic sample contained. In the three sets of control samples (i.e. samples without nanoparticles), mean THM amounts occurred at levels from 1.50×10^{-3} to 1.16×10^{-2} mg/L. The mean THM amounts for the samples dosed with TiO_2 ranged from 2.00×10^{-3} to 1.57×10^{-2} mg/L. Lastly, the mean THM amounts in the ZnO samples were from 1.33×10^{-3} to 1.09×10^{-2} mg/L.

Fig. A.4 (included in Appendix A) shows the average levels of HAAs that each nanoparticle-dosed water contained. Mean HAA amounts for the control samples ranged from 3.30×10^{-3} to 4.30×10^{-2} mg/L. For TiO_2 samples, the mean HAA amounts were 1.40×10^{-3} to 4.70×10^{-2} mg/L. Finally, the mean HAA amounts for ZnO samples occurred in concentrations from 3.27×10^{-3} to 4.38×10^{-2} mg/L.

All water samples dosed with NPs were chlorinated under the same physiochemical conditions. It was expected that a certain amount of DBPs would result from the interactions between free chlorine and the water constituents in each sample. This prediction proved correct, as all samples showed the presence of DBPs, but a statistical analysis indicated that the NPs produced no significant effect ($P>0.05$) on the production of either THMs or HAAs.

3.3.2. Chronic Cell Cytotoxicity Assays

3.3.2.1. CHO-K1 Cellular Assay

The chronic cytotoxic effects of extracts from waters dosed with different NPs on CHO-K1 cells was investigated. Fig. A.5 (included in Appendix A) shows the differences in mean recorded density of CHO-K1 cell cultures after a 72hr exposure period to different sample types (i.e. no dosage, TiO_2, ZnO) over a REF range of $8.0x10^{-3}x$ to 8.0x. Analysis of assay results indicated a statistically significant effect on cytotoxicity when factoring for sample type on its own ($P \geq 0.05$). However, no significant differences in cytotoxicity levels were found after factoring for dilution level and the interaction of these two terms ($P \leq 0.05$). The type of sample, therefore, showed no significant impact on cytotoxicity when accounting for the different dilution levels.

Previous research has indicated that interactions between ENM contaminants and conventional disinfectants can release metal ions. These ions can then go on to interact with NOM (i.e. phenolic moieties and amines) which directly influences DBP generation in source waters (Sharma *et al*., 2017; Zhao *et al*., 2016). Nevertheless, in this study, samples dosed with TiO_2 and ZnO NPs did not demonstrate any significant change in

cytotoxicity in the CHO-K1 assay when compared to samples free of NPs ($P \geq 0.05$). This may be attributed to the concentration of water constituents in the initial water samples, the subsequent low-level generation of DBPs as revealed by the GC/MS chemical analysis, or the low-level dilution concentrations.

3.3.2.2. CaCo-2 Cellular Assay

The chronic cytotoxic effects of synthetic drinking water extracts produced under different disinfectant regimens on CaCo-2 cells was investigated. Fig. 3.1 shows the differences in mean recorded density of CaCo-2 cell cultures after a 72hr exposure period to different sample types (i.e. control, chlorinated, ferrate) over a REF range from $8.0x10^{-3}x$ to 8.0x. A statistical analysis of assay results indicated a significant difference in cytotoxicity levels when factoring for sample type and dilution level, alone. This significance was lost, however, after factoring for the interaction of the two terms. Even so, further analysis showed that ZnO and TiO_2-dosed samples were still significantly more cytotoxic at the 0.8x dilution level when compared to their corresponding control samples.

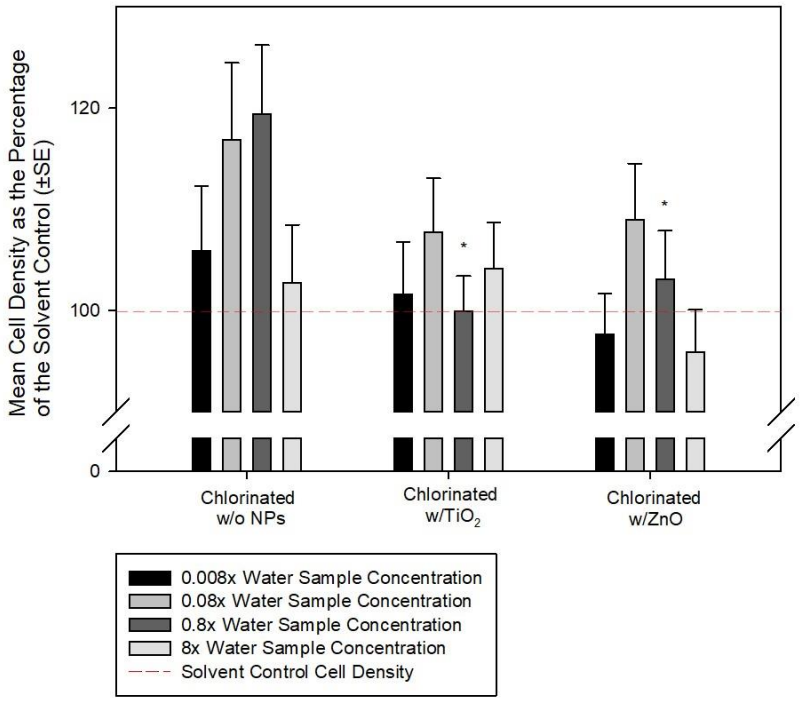

Figure 3.1 Chronic cytotoxicity in human colon (CaCo-2) cells exposed to nanoparticle extracts. CaCo-2 cells were exposed to extracts from synthetic water samples dosed with different types of nanoparticles (no dosage, TiO_2, or ZnO). Values indicate a percentage of the mean recorded cell density for each sample type as compared to the baseline cell density (100%) of the solvent control. A star (*) denotes that the difference in mean values among the indicated sample type is statistically significant compared to the corresponding control sample concentration. A two-way ANOVA test indicated that there was a statistically significant effect on cell density when factoring for extract type and dilution level separately (P = 0.001; P = 0.001). There was no significant effect when factoring the interactive effects of the two terms (P = 0.085). However, a multiple pair-wise comparison (Bonferroni t-test) indicated that extracts from samples dosed with TiO2 and ZnO produced significant decreases in cell density at the 0.8x dilution level when compared to their corresponding control extracts (P = 0.003; P = 0.037).

The CHO-K1 cellular assay did not detect significant changes in cytotoxicity due to ENM exposure in this study. As in the previous chapter, the chemical analysis results indicated that regulated DBP levels in the initial water samples were barely above detection level. Due to the low concentrations of water constituents and high purity of the water, both detected and undetected DBP concentrations were likely too low to

produce significant cytotoxic effects in the CHO-K1 cell culture. In contrast, the CaCo-2 cellular assay appeared slightly more responsive to the differences in NPs used to generate the samples. Potential reasons for this difference include the inherent sensitivities of particular cell lines to toxic insult. The CaCo-2 cell line has a mutation in the p53 gene which might render it more sensitive to certain cytotoxic and genotoxic agents (Liu and Bodmer, 2006). The differences in cytotoxic response between the CHO-K1 assay and the CaCo-2 assay *in vitro* may also stem from differences in the Nrf2-mediated cytoprotection systems inherent between the two species from which the cells originate. These cytoprotection systems can further modify how cells respond to toxic insults (Osburn and Kensler, 2008). Even so, a study by Procházka *et al*. (2015) found that the CaCo-2 cell (MTS) cytotoxicity assay used in their experiments was up to 10-fold less sensitive for tested DBPs than 24 and 72 h CHO and CHO-K1 cytotoxicity assays. The study also asserted that CHO cells tended to exhibit higher sensitivity to the cytotoxic effects of the studied DBPs (HBQs in particular). While these results run counter to this study's findings, it is important to note that Procházka *et al*. (2015) used a methyltetrazolium salt (MTS) cell viability kit for the CaCo-2 cell assay. Also, the assays conducted under Procházka *et al*. (2015) were examining the effects of individual DBP species and not complex DBP mixtures.

3.4. Conclusions

Data from the chemical analyses demonstrated that the addition and UV radiation of either TiO_2 or ZnO NPs in water samples prior to chlorination produced no significant change in concentration of the DBPs under investigation. These results suggest that

while the oxidative interaction between chlorine, NOM moieties, and halides produced a certain amount of the DBPs under investigation, any additional interactions with TiO_2 and ZnO did not catalyze or retard their formation rate. This does not imply that the presence of TiO_2 and ZnO did not impact the formation of other unregulated or unknown DBPs, but that only the DBPs of interest to this study were unaffected.

The CaCo-2 cell line demonstrated a significant increase in cytotoxicity when exposed to ZnO or TiO_2-dosed samples at the 0.8x (REF) concentration level as compared to their corresponding controls. The CHO-K1 cell line, in contrast, showed no significant changes in cytotoxicity after exposure to the different sample types. This discrepancy between cell lines offers insight into potential differences in sensitivity between cells as well as the importance of the p53 gene and/or phase I (i.e. Cytochrome P450 CYP1A1, CYP1A2, CYP2B and CYP2E1), and phase II enzymes (i.e. glutathione-S-transferases, sulfotransferases, N-acteyltransferases, and glucuranosyltransferases) in the CaCo-2 cell line's cytotoxic response toward DBPs. These enzymes (or the active cellular metabolism that they are designed to mimic) may play a critical role in DBP toxicity alongside a cell's sensitivity to DBP insults. Above all, these results highlight a need for additional study on the influence of NPs on the production and toxicity of regulated and unregulated DBPs, as well as more thorough investigations of alternate toxic endpoints.

3.5. References

Dobrovic, S., Juretic, H., Ljubas, D., Vrcek, I., et al. 2012. Genotoxicity and effects of nanosilver contamination in drinking water disinfection. *Water Sci. Technol.* 12, 829–836.

Liu, Y., Bodmer, W. 2006. Analysis of P53 mutations and their expression in 56 colorectal cancer cell lines. *Proc. Natl. Acad. Sci USA.* 103(4):976-981.

Metch, J., Ma, Y., Pruden, A., Vikesland, P. 2015. Enhanced disinfection by-product formation due to nanoparticles in wastewater treatment plant effluents. *Environ. Sci. Water Res. Technol.* 1, 823–831.

Osburn, W.O., Kensler, T.W. 2008. Nrf2 signaling: An adaptive response pathway for protection against environmental toxic insults. *Mut. Res./Rev. Mut. Res.* 659(1):31-39.

Prochazka, E., Escher, B.I., Plewa, M.J., Leusch, F.D.L. 2015. In vitro cytotoxicity and adaptive stress responses to selected haloacetic acid and halobenzoquinone water disinfection byproducts. *Chem. Res. Toxicol.* 28(10).

Sharma, V., Yang, X., Cizmas, L., McDonald, T. J., et al. 2017. Impact of metal ions, metal oxides, and nanoparticles on the formation of disinfection byproducts during chlorination. *Chem. Eng. J.*, 317, 777-792.

Tugulea, A., Bérubé, D., Giddings, M., Lemieux, F., et al. 2014. Nano-silver in drinking water and drinking water sources: stability and influences on disinfection by-product formation. *Environ. Sci. Pollut. Res. Int.* 21, 11823–11831.

Yuan, Z., Li, J., Cui, L., Xu, B., Zhang, H., & Yu, C.. 2013. Interaction of silver nanoparticles with pure nitrifying bacteria. *Chemosphere.* 90, 1404–1411.

Zhao, Y., Yang, H., Liu, S., Tang, S., Wang, X., Xie, Y.F. 2016. Effects of metal ions on disinfection byproduct formation during chlorination of natural organic matter and surrogates. *Chemosphere*. 144:1074-1082.

4. ASSESSING AND COMPARING HUMAN BIOASSAY SENSITIVITIES FOR CYTOTOXICITY, ROS GENERATION, AND AUTOPHAGY FOLLOWING EXPOSURE TO COMPLEX DISINFECTION BYPRODUCT MIXTURES

4.1 Introduction

At present, a small subset of disinfection byproduct (DBP) studies have attempted to characterize the effects of specific DBPs or DBP classes on cell viability, reactive oxygen species (ROS) generation, and autophagy among relevant human cell lines (Chen, 2019; Pals, 2013; Wang, S., 2014). There are, however, no such studies examining the role of alternative disinfection regimens [i.e. ferrate(VI)] or the presence of engineered nanomaterials (ENMs) in the formation of complex DBP mixtures that produce these potentially harmful effects. In absence of any established literature, there is a need to assess the influence of these precursors by comparing differences among cytotoxicity, reactive oxygen species (ROS) generation, and autophagy produced from their respective yield of DBPs across a variety of human cell lines.

To fill each gap in knowledge and further capture the full range of potential toxic effects produced by complex DBP mixtures, three *in vitro* bioassays were employed. The CellTiter-Glo® Luminescent Cell Viability Assay, the OxiSelect™ Intracellular ROS Assay Kit, and the LentiBrite™ Lentiviral Biosensor Assay examined the effects of DBP mixtures on cytotoxicity, ROS, and autophagy levels, respectively, across three relevant human cell lines. These cell lines included human embryonic kidney cells

[HEK-293 (ATCC® CRL-1573™)], human gastric epithelium cells (GES-1), and human fetal colon cells [FHC (ATCC® CRL-1831™)]).

The CellTiter-Glo® Luminescent Cell Viability Assay quantifies cytotoxicity levels in a cell culture. It does so by measuring the luminescent signal generated by luciferase in direct proportion to the amount of ATP and the number of healthy cells in a culture. This assay was selected because it is designed for use with multiwell-plate formats, produces a highly stable luminescent signal, and can detect as few as 15 cells per well which makes it ideal for the accurate quantification of cell proliferation and cytotoxicity (Beerli, *et al.* 2015; Enayetallah, *et al.* 2013; Yang *et al.* 2015). The CellTiter-Glo® Luminescent Cell Viability Assay has also been used for similar purposes in other studies, such as Lv, *et al.* (2017) which used it to evaluate cytotoxicity levels in CHO-K1 cells exposed to chlorinated and solar-treated reclaimed water samples. Similarly, Yang *et al.* (2015) employed the CellTiter-Glo® Luminescent Cell Viability Assay to evaluate cytotoxicity levels in human liver hepatoma (HepG2) cells exposed to dissolved organic matters (DOMs) of secondary effluents and found that it showed a more stable dose-response relationship compared to the conventional 3-(4,5-Dimethylthiazol-2-yl)-2,5-diphenyltetrazolium bromide (MTT) assay.

The OxiSelect™ Intracellular ROS Assay Kit quantifies ROS levels in a cell culture through a fluorogenic probe 2', 7'-Dichlorodihydrofluorescin diacetate (DCFH-DA), which diffuses into cells and is deacetylcated by cellular esterases into the non-fluorescent 2', 7'-Dichlorodihydrofluorescin (DCFH). In the presence of ROS, DCFH is rapidly oxidized to highly fluorescent 2', 7'-Dichlorodihydrofluorescein (DCF). The

ensuing fluorescence is then read as a surrogate for ROS levels by a plate reader. This assay was selected because it is compatible with 96 well-plate formats, uses a quick 1hr protocol, and is highly sensitive to ROS levels as low as 10 pM (Du *et al.*, 2020; Eruslanov & Kusmartsev, 2010; Raez-Villanueva, *et al.*, 2019). The OxiSelect™ Intracellular ROS Assay (or analogous assays) has already been used for similar purposes in other studies. Hung *et al*. (2019), for instance, used a DCFH-DA probe to examine the effect of 2,6-dichloro-1,4-benzoquinone (DCBQ) on ROS generation in normal human colon cells (CCD 841 *CoN*) and human liver cancer cells (HepG2). Another study by Li *et al.* (2016) used a DCFH-DA probe to quantify ROS levels produced by eight HBQs in CHO-K1 cells.

The LentiBrite™ Lentiviral Biosensor assay allows *in vitro* imaging of autophagosomes in mammalian cell lines. This assay was selected for its comparatively high transfection efficiency, its ability to transfect a variety of human cell types, and for its inobtrusive impact on routine cellular function. Other studies have used the LentiBrite™ Lentiviral Biosensor assay (or equivalent assays) for similar ends. Liao, *et al.* (2020), for instance, used a lentiviral vector to assess autophagy levels in a human hepatoma (Huh7) cell line exposed to the compound deguelin. Another study by Jin, *et al.* (2019) employed a GFP-LC3 lentiviral vector to assess autophagy levels in mammalian macrophage cells (i.e. Raw264.7 and Ana-1) exposed to iron oxide nanoparticles.

The objectives of this study were (1) to assess the effects of DBP mixtures generated under different disinfectant methods [i.e. no disinfectant, Fe(VI), or

chlorination] on cell viability, ROS generation, and autophagy in HEK-293, GES-1, and FHC cells; and (2) to assess the effects of DBP mixtures generated in the presence of nanomaterial precursors (i.e. no NPs, TiO_2, or ZnO) on cell viability, ROS generation, and autophagy in HEK293, GES-1, and FHC cell lines. It was hypothesized Fe(VI)-treated waters would be less cytotoxic, produce less ROS, and lower autophagy levels than the chlorinated samples across all cell lines. It was also hypothesized that NP-dosed waters would be more cytotoxic, produce more ROS, and higher autophagy levels than the NP-free control samples across all cell lines.

4.2 Materials & Methods

4.2.1 Chemicals & Reagents

As specified in the previous two chapters (Sections 2.2.1. and 3.2.1.) reagents were certified ACS reagent grade and were purchased from Fisher Scientific (Itasca, IL) and Sigma-Aldrich (St. Louis, MO) (See Appendix B, Table 1 for details). Potassium iodide (KI), sodium bromide (NaBr), TiO_2, and ZnO nanoparticles were purchased from Fisher Scientific (Itasca, IL) and Sigma-Aldrich (St. Louis, MO). Suwanee River natural organic matter (NOM) was purchased from the International Humic Substances Society (IHSS; St. Paul, MN). F-12K media, fetal bovine serum (FBS), EDTA-trypsin, and penicillin/streptomycin mixtures were purchased from the American Type Culture Collection (ATCC; Manassas, VA). Oasis HLB cartridges (6 cc, 150 mg, 30 μm particle size) were purchased from Waters (Milford, MA). All solvents [acetonitrile, n-hexane, methanol, dimethyl sulfoxide (DMSO)] were of highest purity and were purchased from Fisher Scientific (Itasca, IL), Sigma-Aldrich (St. Louis, MO), or VWR International

(Radnor, PA). Chemical properties, purity, and CAS numbers of all compounds are provided in Table 1 (Appendix B).

4.2.2 Preparation of Water Samples

Synthetic water mixtures were prepared according to previous chapters (Sections 2.1.2. and 3.1.2.). Synthetic water samples consisted of ultra-pure Milli-Q water, NOM, potassium iodide (KI), sodium bromide (NaBr), and either phosphate buffer or MES hydrate. After pH adjustment, filtration, and a 24 hour stir period, the samples were either dosed with NPs [TiO_2, ZnO, or no NPs (control)] and then chlorinated, or directly treated with different disinfectants [(chlorine, ferrate, or left untreated (control)]. Upon treatment, the samples were put in a dark area under long-wave (365 nm) UV lights for 2hrs and then allowed to stir for an additional 48hr period. A small portion of each sample was removed for chemical analysis.

4.2.3 Concentration of the Extract

The remaining sample volumes were pre-concentrated by solid phase extraction (SPE) using Oasis HLB cartridges according to a procedure described in the previous chapters (Sections 2.2.3. and 3.2.3.). The extracted samples then underwent elution, dehydration, and concentration/solvent exchange procedures as described in the previous chapters (Sections 2.2.2. and 3.2.2.). The final product was a water sample extract with an 8000x concentration factor (CF) compared to the original sample.

4.2.4 Chemical Analyses

A portion of each water sample was collected, stored, and shipped to Alexin Analytical Laboratories (Tigard, OR), a NELAP accredited lab, for DBP

(TTHM/HAA5) analysis by gas chromatography/mass spectrometry (GC/MS) determination according to the same methods described in the previous chapters (Sections 2.2.4. and 3.2.4.). All analyses were conducted according to EPA Methods 524.2 (TTHM; Revision 4.1) and 552.1 (HAA5; Revision 1.0) (see sections 9 & 10 of each method for quality control and calibration measures).

4.2.5 Human Cell Lines

Three different human cell lines were used for the cellular assays employed during this study: human embryonic kidney cell line HEK-293 (ATCC® CRL-1573™), human gastric epithelial cell line GES-1 (ATCC® CRL-1573™), and normal human fetal colon cell line FHC (ATCC® CRL-1831™). Using the same procedures described in the previous two chapters (Sections 2.2.5. and 3.2.5.), all cells were maintained in complete growth media. The complete growth media consisted of F-12K medium, 5% fetal bovine serum (FBS), and 1% antibiotics (100 U/mL sodium penicillin G, 100 μg/mL streptomycin sulfate) at 37 °C in a humidified atmosphere of 5% CO_2.

4.2.6 Cell Viability Assay

The CellTiter-Glo® Luminescent Cell Viability Assay measures cytotoxicity in a culture based on quantitation of the ATP present. The amount of ATP is directly proportional to the number of metabolically active cells in a cell culture. A reagent (CellTiter-Glo® Reagent) was added directly to a 96-well plate HEK-293 cell culture exposed to a range of drinking water sample concentrations. The resulting cell lysis produced a luminescent signal proportional to the amount of ATP present in each well, which was then analyzed by microplate reader. The individual assays were repeated 3

times and the resulting data points were averaged into mean absorbance values. The mean blank-corrected absorbance values of the negative control (cells with media only) were subtracted from the mean absorbance of each treatment group. The corrected mean absorbance value for each treatment group was then converted into a percentage of the mean absorbance obtained from the corresponding solvent control in order to provide the graphs more consistency.

4.2.7 Reactive Oxygen Species (ROS) Generation Assay

The OxiSelect™ Intracellular ROS Assay Kit measures ROS generation in cells based on the fluorescence intensity of a cell-permeable fluorogenic probe when compared to a dichlorodihydrofluorescein (DCF) standard. This assay employs a cell-permeable fluorogenic probe 2', 7'-Dichlorodihydrofluorescin diacetate (DCFH-DA) to quantify hydroxyl, peroxyl, or other ROS activity in a cell based on its fluorescence intensity when compared to a dichlorodihydrofluorescein (DCF) standard. DCFH-DA and a DCF standard were added directly to 96-well plates of either HEK-293, GES-1, or FHC cell cultures and then exposed to a high-level sample concentration (8.0x REF). After incubation, the cell plates were read on a fluorescence plate reader and the DCFH-DA results were compared to the DCF standard results. Each assay was repeated 3 times and the resulting data points of each treatment column were averaged into mean absorbance values. The mean absorbance value of the negative control (cells with media only) was subtracted from the mean absorbance value of the treatment group. The corrected mean absorbance for each treatment group was then converted into a

percentage of the mean absorbance value obtained from the corresponding solvent control in order to provide the graphs with greater consistency.

4.2.8 Autophagy Assay

LentiBrite™ Lentiviral Biosensors were employed to measure and view autophagy in cell lines. The assay's biosensors fuse TagGFP2 and TagRFP at their C-termini to the autophagosome marker LC3. LC3 precursors, distributed in the cytosol, are processed to form LC3-I. During autophagy, the C-terminal glycine is modified by addition of a phosphatidylethanolamine to form LC3-II, which translocates to autophagosomes in a punctate distribution. This translocation process provides a bright fluorescence and precise localization of autophagosomes in cell cultures. 26-well plates of either HEK-293 cell cultures were exposed to a high-level sample concentration (8.0x REF). After the exposed cells had seeded over a 48hr period, appropriate volumes of diluted lentiviral stock were added to the plates and incubated for an additional 24hr period. The lentivirally transduced cells were then imaged by a wide-field fluorescent microscope to detect the cytoplasmic accumulation of autophagic vacuoles (AVO).

4.2.9 Statistical Analyses

For the cell viability assays, one-way ANOVA tests were conducted to determine if the samples induced a statistically significant level of cytotoxicity compared to the control samples of corresponding dilution levels. For the ROS assays, one-way ANOVA tests were conducted to determine if the samples induced a statistically significant level of ROS generation. If a significant F value ($P \leq 0.05$) was obtained in the former, a pair-wise multiple comparison analysis (Bonferroni t-test) was performed. For the latter, a

Holm-Sidak multiple comparison was preformed between group pairs. The power of the test statistic ($1-\beta$) for both assays was maintained as ≥ 0.8 at $\alpha = 0.05$.

4.3 Results

4.3.1 Chemical Analysis

The effect of disinfectants on the production of regulated THMs and HAAs in synthetic drinking water samples was investigated by GC/MS analysis. Mean THM and HAA amounts from different disinfection regimens and NP types are reported in the two previous chapters (Sections 2.2.1., 3.2.1.). To summarize, only chlorinated samples produced a small amount (2.30×10^{-3} to 3.36×10^{-2} mg/L) of regulated THMs and HAAs out of the three different disinfectant sample types. Neither the control (non-disinfected water) samples nor the samples treated with Fe(VI) were found to generate any of the THMs or HAAs assessed in this study. For the three sample types dosed with different NPs, mean THM and HAA amounts ranged from 1.33×10^{-3} to 4.70×10^{-2} mg/L. The difference in the mean values among the different types of NP-dosed samples were not statistically significant in terms of their effects on the production of either THMs or HAAs examined in this study when compared to the control samples ($P \geq 0.05$).

4.3.2 Cell Viability Assay

The impact of samples generated under different disinfectant regimens or NP dosages on human cell viability was investigated using the CellTiter-Glo® Luminescent Cell Viability Assay. Figs. 4.1 and 4.2 along with A.6 to A.9 (included in Appendix A) show the mean cell densities (as a percentage of the mean negative control ±SE) of

HEK293, GES-1, and FHC cell cultures exposed to various samples over a range of concentrations.

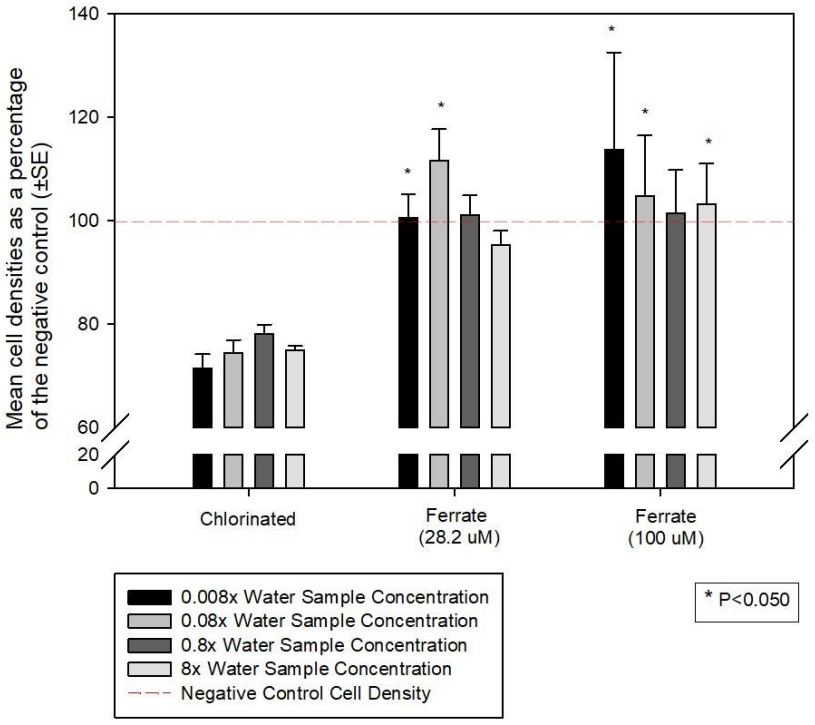

Figure 4.1 Cell viability for HEK293 cells exposed to disinfectant extracts. Cell viability assay results from human kidney (HEK293) cells exposed to water extracts from synthetic water samples treated under different disinfectant regimens. Values indicate a percentage of the mean recorded cell density for each sample type as compared to the baseline cell density (100%) of the solvent control. A star (*) denotes that the difference in mean values among the indicated disinfectant group is statistically significant compared to the corresponding control group. A one-way ANOVA indicated a statistically significant difference in the mean values among the different extract types after allowing for differences in concentration level (P = <0.001). A pair-wise multiple comparison (Bonferroni t-test) indicated that ferrate(VI) (100 uM) had significantly higher cell densities at dilution levels $8.0E^{-3}$, $8.0E^{-2}$, and 8.0 (P = <0.001; P = 0.005; P=0.011) compared to HEK293 cell cultures exposed to corresponding dilutions of chlorinated extracts. Ferrate(VI) (28.2 uM) had significantly higher cell densities at sample concentrations $8.0E^{-3}$ (P=0.007) and $8.0E^{-2}$ (P=<0.001).

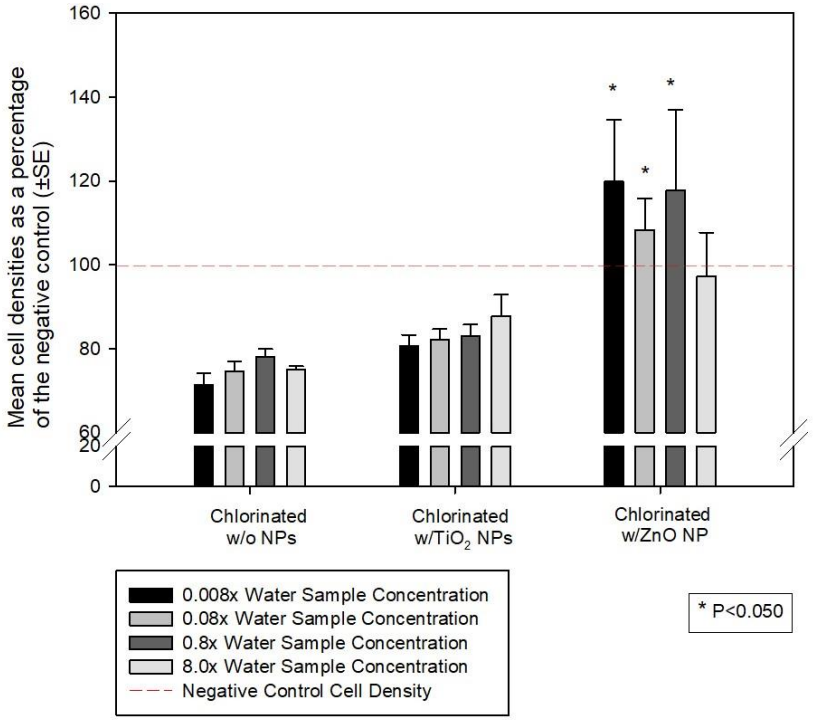

Figure 4.2 Cell viability assay for HEK293 cells exposed to nanoparticle extracts. Cell viability assay results from human kidney (HEK293) cells exposed to water extracts from synthetic water samples treated under different disinfectant regimens. Values indicate a percentage of the mean recorded cell density for each sample type as compared to the baseline cell density (100%) of the solvent control. A star (*) denotes that the difference in mean values among the indicated disinfectant group is statistically significant compared to the corresponding control group concentration. A one-way ANOVA indicated that the difference in the mean values among the different extract types is statistically significant (P = <0.001). A pair-wise multiple comparison (Bonferroni t-test) indicated that cell cultures exposed to drinking water extracts dosed with ZnO at concentration levels $8.0E^{-3}$ (P=<0.001), $8.0E^{-2}$ (P=0.002), and $8.0E^{-1}$ (P=<0.001) had significantly higher densities than the HEK293 cell cultures exposed to corresponding concentrations of extracts w/o NPs.

HEK293 cell cultures exposed to samples disinfected with 28.2 uM of Fe(VI) had significantly lower levels of cytotoxicity than the HEK293 cell cultures exposed to the chlorinated samples at certain dilution levels ($8.00x10^{-3}$ and $8.00x10^{-2}$). Exposure to samples disinfected with 100 uM of Fe(VI) produced significantly lower levels of cytotoxicity when compared to cells exposed to chlorinated samples at certain dilution

levels ($8.00x10^{-3}x$, $8.00x10^{-2}x$, and 8.00x). HEK293 cell cultures exposed to samples dosed with ZnO showed significantly lower levels of cytotoxicity compared to cells exposed to control samples at certain dilution levels ($8.00x10^{-3}$, $8.00x10^{-2}$, $8.00x10^{-1}$). Exposing GES-1 cells to samples from disinfected waters and waters dosed with NPs, however, produced no significant change in cytotoxicity levels compared to the control samples. FHC cells showed significant differences in cytotoxicity levels between cells exposed to samples disinfected with 28.2 or 100 uM of Fe(VI) or samples dosed with NPs when compared to cells exposed to control samples. However, further statistical analyses showed no significant differences in cytotoxicity once the samples were compared across corresponding dilution levels.

The above findings suggest that exposure to samples disinfected with Fe(VI) allow for significantly lower levels of cytotoxicity than their chlorinated counterparts across the HEK293 cell line. Since waters disinfected with Fe(VI) produced none of the THMs or HAAs assessed in this study, the absence of their additional cytotoxic effects may help promote cellular growth. However, since this response was only seen in HEK293 cells, it may be that the other two cell lines (along with CHO-K1 and CaCo-2 cells from the previous chapters) are not as sensitive to the cytotoxic insults produced from the low levels of DBPs assessed in this study.

GC/MS chemical analysis demonstrated that the addition of TiO2 and ZnO NPs did not significantly increase tested DBP levels in drinking water samples. TiO_2-dosed water samples were not shown to significantly impact cytotoxicity levels across the three cell lines as compared to control samples disinfected with chlorine (Figs 4.2, A.5, A.7.

A.9). The decrease in cytotoxicity among HEK293 cells exposed to ZnO-dosed samples may have been due to the photocatalytic oxidative properties of ZnO which could enhance the biodegradation rate of select organic contaminants. The HEK293 cell line may be particularly susceptible to these organics, which may outweigh the cytotoxic burden of any additional DBPs.

4.3.3. ROS Generation Assay

The impact of disinfectant regimens or NP dosages on ROS generation in human cells was investigated using the OxiSelect^{TM} Intracellular ROS Assay Kit. Figs. 4.3 to 4.5 and A.10 to A.12 (included in Appendix A) show the ratio between the DCFH count and the mean live cell concentration (MLCC) (as a percentage of the negative control ±SE) of cells exposed to various samples at a 8.00x relative enrichment factor (REF).

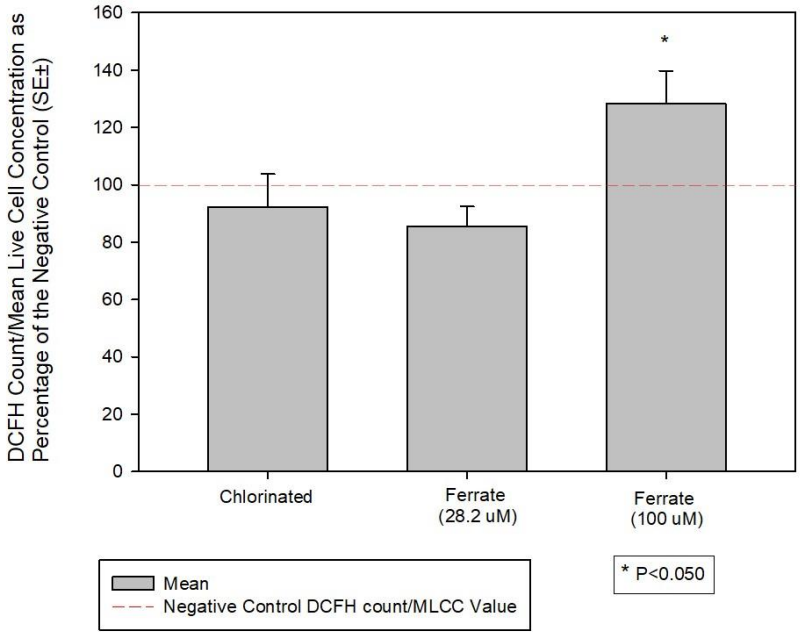

Figure 4.3. ROS assay for GES-1 cells exposed to disinfectant extracts. ROS assay results from human gastric epithelial (GES-1) cells exposed to water extracts from synthetic water samples treated under different disinfectant regimens. Values indicate a ratio of the mean recorded DCFH Count/Mean Live Cell Concentration (MLCC) as a percentage of the baseline (100%) negative control value. A star (*) denotes that the difference in mean values among the indicated disinfectant group is greater than would be expected by chance. A one-way ANOVA revealed that the differences in the mean values among the extract types are statistically significant (P = 0.004). A pair-wise multiple comparison (Bonferroni t-test) indicated that cells exposed to extracts from drinking water samples disinfected with 100 uM of ferrate(VI) showed significantly higher DCFH Count/Mean Live Cell Concentration (MLCC) values than cells exposed to extracts from drinking water samples disinfected with chlorine (P = 0.015) and 28.2 uM of ferrate(VI) (P = 0.006).

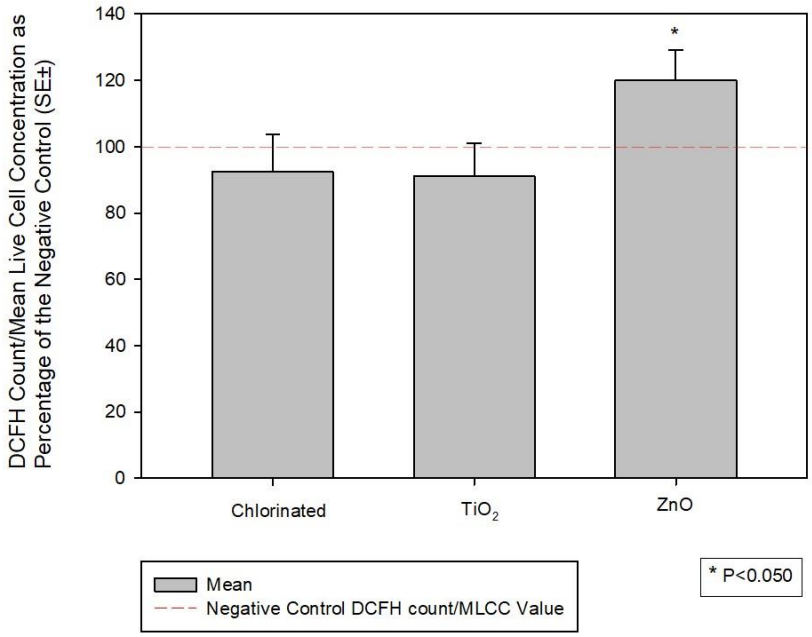

Figure 4.4 ROS assay for GES-1 cells exposed to nanoparticle extracts. ROS assay results from human gastric epithelial (GES-1) cells exposed to water extracts from synthetic water samples treated under different microcontaminant regimens. Values indicate a ratio of the mean recorded DCFH Count/Mean Live Cell Concentration (MLCC) as a percentage of the baseline (100%) negative control value. A star (*) denotes that the difference in mean values among the indicated disinfectant group is greater than would be expected by chance. A one-way ANOVA revealed that the differences in the mean values among the extract types are statistically significant (P = 0.021). A pair-wise multiple comparison (Bonferroni t-test) indicated that cells exposed to extracts from drinking water samples dosed with ZnO showed significantly higher DCFH Count/Mean Live Cell Concentration (MLCC) values than cells exposed to extracts from drinking water samples disinfected with chlorine (P = 0.047) and those dosed with TiO_2 (VI) (P = 0.039).

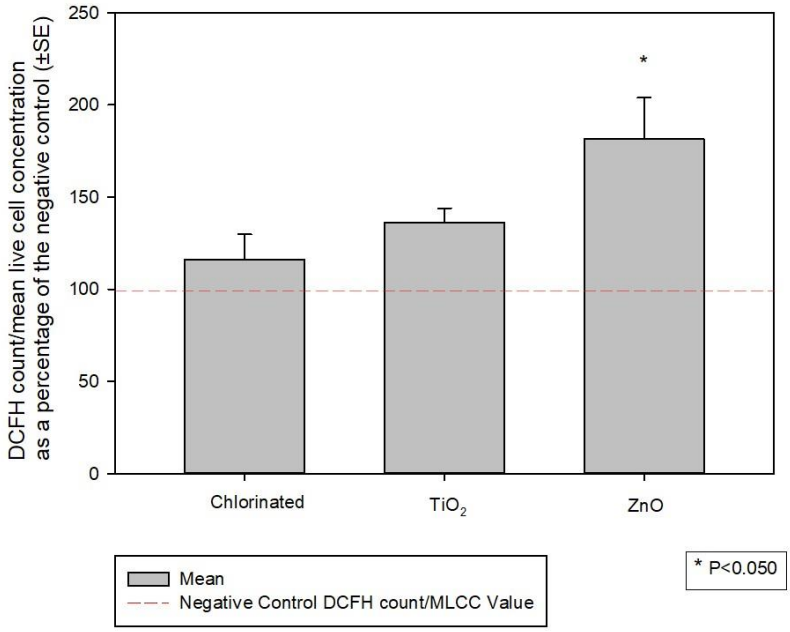

Figure 4.5 ROS assay for FHC cells exposed to nanoparticle extracts. ROS assay results from human fetal colon (FCH) cells exposed to water extracts from synthetic water samples treated under different microcontaminant regimens. Values indicate a ratio of the DCFH count/mean live cell concentration as a percentage of the baseline value (100%) of the negative control. A star (*) denotes that the difference in mean values among the indicated disinfectant group is greater than would be expected by chance. A one-way ANOVA revealed that the differences in the mean values among the extract types are statistically significant (P = 0.006). A pair-wise multiple comparison (Bonferroni t-test) revealed that cells exposed to extracts from drinking water dosed with ZnO had significantly higher DCFH count/MLCC values than cells exposed to chlorinated drinking water extracts (P = 0.007) and cells exposed to TiO_2-dosed drinking water extracts (P = 0.038).

The mean ROS levels in HEK293 cells exposed to Fe(VI) or chlorinated samples were not statistically significant compared to the values seen in the control samples. Likewise, HEK293 cells exposed to water samples dosed with different NPs indicated that the differences in ROS levels were also not statistically significant. As such, none of the sample types had any significant effect on ROS generation in HEK293 cell cultures.

In contrast, the differences ROS levels after exposure to samples produced with different disinfectants were statistically significant in GES-1 cells compared to the

control samples. Samples disinfected with 100 uM of Fe(VI) had significantly higher ROS levels than cell cultures exposed to drinking water disinfected with 28.2 uM of Fe(VI) or chlorine. Cells exposed to samples dosed with ZnO had significantly higher ROS levels than GES-1 cells exposed to samples disinfected with chlorine or samples dosed with TiO_2.

Differences in ROS levels among FHC cells exposed to samples generated under different disinfectants were not significant. However, ROS levels among FHC cells exposed to samples dosed with different NPs were significant. Samples dosed with ZnO had significantly higher ROS levels than cells exposed to samples disinfected with chlorine or samples dosed with TiO_2.

The above results suggest that GES-1 and FHC cells are more sensitive to changes in ROS generation after exposure to the various samples as compared to the HEK293 cells. Results also suggest that GES-1 cells exposed to samples disinfected with a high level of Fe(VI) (100 uM) or dosed with ZnO produced significantly higher ROS levels than other samples. FHC cells, in comparison, only produced significantly more ROS levels upon exposure to samples dosed with ZnO. DBPs are known to induce mitochondrial damage to susceptible cells which increases the generation of intracellular ROS (Cortés & Marcos, 2018; Dad *et al*., 2013; Pals *et al*., 2013). However, samples disinfected with Fe(VI) were found to produce none of the DBPs under investigation, and samples dosed with ZnO were found to produce no significant increase in DBPs under investigation compared to samples disinfected with chlorine or samples dosed with TiO_2 after chemical analysis. According to a study by Escher *et al*. (2013), an

oxidative stress response is relatively nonspecific when addressing possible sources of toxic action, with a wide variety of chemicals producing ROS directly or indirectly, as well as inducing Nrf2 activation. Evidence of an oxidative stress response, then, is not necessarily indicative of a toxic effect, but serves as an early warning indicator of potential adverse effects. It is only when oxidative stress levels in a cell outstrip the capabilities of its defense mechanisms to compensate that apoptosis and necrosis ensue. Since the recorded ROS levels appeared to have no discernable impact on overall cell viability in their respective cell cultures [Fe(VI) and ZnO-dosed samples were shown to either increase or have no effect on cell densities in the cell viability assays], it is unlikely that any of the significant ROS levels recorded by the assay indicated an actual source of toxic action in the GES-1 and FHC cells.

4.3.4. Autophagy Assay

The impact of samples generated under different disinfectant regimens and NP dosages on AVOs in human cells was investigated by the LentiBrite™ Lentiviral Biosensor assay. Figs. A.13 to A.17 (included in Appendix A) show fixed HEK293 cells with florescent markers that identify the cytoplasmic sites of AVO accumulation in cells exposed to samples formed under different disinfectant and microcontaminant regimens. Table 2 (included in Appendix B) displays the mean number of punctuates per cell found for each sample type. Overall, HEK293 cell cultures showed minor variation in autophagy between samples, with a range of 1 to 3.5 punctuates per cell. The low level of AVOs suggests low levels of cellular stress in all cultures regardless of exposure to the various sample types under study.

There could be a number of reasons for the detection of such low levels of cellular stress. As with many of the previous assays showing little to no significant results, these findings may stem the fact that the added amounts of reactants and water constituents were intended to mimic average levels observed in natural surface waters. Hence, the degree of DBP production may have been too low under these conditions to produce a significant response from conventional cellular assays.

4.4. Conclusions

According to the cytotoxicity results, samples treated with Fe(VI) at certain dilution levels, across both high and low dosages [28.2 uM (0.008x, 0.08x) and 100 uM (0.008x, 0.08x, 8.0x), respectively] and samples dosed with ZnO (0.008x, 0.08x, 0.8x) produced significant decreases in cytotoxicity levels when compared to the corresponding control sample, but not among GES-1 or FHC cells. The data offer further evidence for Fe(VI)-treated samples as either superior to (in the case of HEK293 cells) or, at the very least, equivalent (in the case of GES-1 and FCH cells) in their impact on overall cytotoxicity compared to conventional chlorinated disinfectants. The differences in cytotoxic response between the three cells types also offers some insights into their relative sensitivity to DBP mixtures and the complexities surrounding their potential toxic endpoints.

Data from the ROS generation assay indicate that at a high dosage of Fe(VI) at the highest dilution level (8.0x) produced a significant increase in ROS levels in GES-1 cells compared to the chlorinated control sample. ZnO-dosed samples at the highest dilution level also produced a significant increase in ROS levels in GES-1 and FHC cells

compared to the control. These results suggest that, at high enough levels, Fe(VI) may contribute to a large spike in ROS levels among certain cells types due to its role as a powerful oxidizer. Likewise, ZnO's photocatalytic oxidative properties may have played a role in promoting ROS generation in the two cell lines. The presence of heightened ROS levels, however, did not correspond with any increases in DBP formation in the samples or have any adverse effect on cytotoxicity levels in the cellular assays. Accordingly, the ROS levels are likely more indicative of a generalized cellular reaction to the presence of these compounds or other unexamined byproducts rather than an active indication of cellular toxicity. The differences in ROS levels between cell types, though, provides some helpful information on their relative sensitivities.

Results from the autophagy assay indicated a low number of AVOs in the exposed HEK293 cells, indicating a minimal degree of cellular stress regardless of sample type. While this outcome does not provide any direct indication of a specific cellular response, it still provides some relevant evidence that autophagy plays a limited role in DBP toxicity. Consequently, these results help to narrow the wide range of toxic endpoints that should be considered when investigating complex DBP mixtures.

Overall, these findings offer important information regarding the impact of Fe(VI) and ZnO on cell viability in HEK293 cells. It also presents some useful points of comparison regarding DBP sensitivity between a variety of human cell lines and biological assays, giving direction and focus to future research projects. Finally, it suggests a need for further exploration into the formation and cytotoxic effects of

complex DBP mixtures, additional in-depth characterizations, and their toxic endpoints in humans.

4.5. References

Attene-Ramos, M. S., Wagner, E. D., Plewa, M. J. 2010. Comparative human cell toxicogenomic analysis of monohaloacetic acid drinking water disinfection byproducts. *Env. Sci. Tech.* 44, 7206−7212.

Aykin-Burns, N., Ahmad, I., Zhu, Y., Oberley, L., Spitz, D. 2009. Increased levels of superoxide and H2O2 mediate the differential susceptibility of cancer cells versus normal cells to glucose deprivation. *Biochem J.* 418(1):29.

Beerli, R.R., Hell, T., Merkel, A. S., Grawunder, U. 2015. Sortase enzyme-mediated generation of site-specifically conjugated antibody drug conjugates with high in vitro and in vivo potency. *Plos One.* 10(7)

Chen, Y., Xu, T., Yang, X., Chu, W., Hu, S., Yin, D. 2019. The toxic potentials and focus of disinfection byproducts based on the human embryonic kidney (HEK293) cell model. *Sci. Tot. Env.* 664:948-957.

Cortésa, C., Marcos, R. 2018. Genotoxicity of disinfection byproducts and disinfected waters: A review of recent literature. *Mut. Res./Gen. Tox. Env. Mut.* 831, 1-12.

Cui, J., Liu, J., Wu, S., Wang, Y., Shen, H., et al. 2013. Oxidative DNA damage is involved in ochratoxin A-induced G2 arrest through ataxia telangiectasia-mutated (ATM) pathways in human gastric epithelium GES-1 cells in vitro. *Arch Toxicol.* 87(10):1829-1840.

Cusick, J., Mustian, A., Goldberg, K., & Reyland, M. 2010. RELT induces cellular death in HEK 293 epithelial cells. *Cell. Immun.* 261(1), 1-8

Dad, A., Jeong, C.H., Pals, J.A., Wagner, E.D., & Plewa, M.J. 2013. Pyruvate remediation of cell stress and genotoxicity induced by haloacetic acid drinking water disinfection by-products. *Environ. Mol. Mutagen.* 54(8):629-637.

Du, Y., Wang, W., He, T., Sun, Y., Lv, X., Wu, Q., & Hu, H. 2020. Chlorinated effluent organic matter causes higher toxicity than chlorinated natural organic matter by inducing more intracellular reactive oxygen species. *Sci. Total Env.* 701.

Enayetallah, A.E., Puppala, D., Ziemek, D., Fischer, J.E., Kantesaria, S., et al. 2013. Assessing the translatability of in vivo cardiotoxicity mechanisms to in vitro models using causal reasoning. *BMC Pharmacol. Toxicol.* 14, 46.

Eruslanov, E. & Kusmartsev, S. 2010. Identification of ROS using oxidized DCFDA and flow-cytometry. In: Armstrong, D. (Eds) Advanced protocols in oxidative stress II. *Methods Molecular Bio.* 594. Humana Press, Totowa, NJ.

Escher, B.I., van Daele, C., Dutt, M., Tang, J.Y.M., Altenburger, R. 2013. Most oxidative stress response in water samples comes from unknown chemicals: The need for effect-based water quality trigger values. *Env. Sci. Tech.* 47(13):7002-7011.

Jin, R., Liu, L., Zhu, W., Li, D., Yang, L., et al. 2019. Iron oxide nanoparticles promote macrophage autophagy and inflammatory response through activation of toll-like receptor-4 signaling. *Biomat.* 203, 23-30.

Li, J., Bauer, M., Moe, B., Leslie, E. M., Li, X., et al. 2017. Multidrug resistance protein 4 (MRP4/ABCC4) protects cells from the toxic effects of halobenzoquinones. *Chem. Res. Tox.* 30(10), 1815-1822.

Lian, H., Cui, J., Wang, Y., Liu, J., Wang, J., et al. 2014. Downregulation of Rad51 participates in OTA-induced DNA double-strand breaks in GES-1 cells in vitro. *Tox. Letters.* 226(2):214-221.

Liao, W., Liu, X., Yang, Q., Liu, H., Liang, B., et al. 2020. Deguelin inhibits HCV replication through suppressing cellular autophagy via down regulation of Beclin1 expression in human hepatoma cells. *Antivi. Res.* 174.

Lv, X., Zhang, X., Du, Y., Wu, Q., Lu, Y., *et al*. 2017. Solar light irradiation significantly reduced cytotoxicity and disinfection byproducts in chlorinated reclaimed water. *Water Research.* 125, 162-169

Pals, J., Attene-Ramos, M. S., Xia, M., Wagner, E. D., Plewa, M. J. 2013. Human cell toxicogenomic analysis linking reactive oxygen species to the toxicity of monohaloacetic acid drinking water disinfection byproducts. *Env. Sci. Tech.*, 47 (21), 12514-12523.

Raez-Villanueva, S., Jamshed, L., Ratnayake, G., Cheng, L., Thomas, P.J., Holloway, A.C. 2019. Adverse effects of naphthenic acids on reproductive health: A focus on placental trophoblast cells. *Reprod. Toxicol.* S0890-6238(19)30313-2.

Stepanenko, A., & Dmitrenko, V. 2015. HEK293 in cell biology and cancer research: Phenotype, karyotype, tumorigenicity, and stress-induced genome-phenotype evolution. *Gene.* 569(2), 182-190.

Wang, S., Zheng, W., Liu, X., Xue, P., Jiang, S., et al. 2014. Iodoacetic acid activates nrf2-mediated antioxidant response in vitro and in vivo. *Env. Sci. Tech.* 48 (22), 13478-13488.

Yang, Y., Lu, Y., Wu, Q., Hu, H., Chen, Y., *et al*. 2015. Evidence of ATP assay as an appropriate alternative of MTT assay for cytotoxicity of secondary effluents from WWTPs. *Ecotox. Env. Safety.* 122, 490-496.

5. CONCLUSIONS

DBPs are of growing concern to drinking water safety. As sources of potable water become increasingly strained from the combined pressures of overconsumption, pollution, and the effects of global climate change, the use/reuse of marginal-quality resources will likely become an essential tool in meeting mounting demands. Such waters, however, are naturally rich in a variety of DBP precursors (i.e. halides, NOM, emerging contaminants). Mass treatment using conventional chemical disinfectants such as free chlorine and chloramine will exacerbate the formation of toxic DBP mixtures in drinking water under such conditions, with major implications for public health as a result. Accordingly, further explorations into DBP formation and the various cytotoxic effects of unknown DBP mixtures are necessary prior to these impending shifts in water management strategies. Continual evaluations on the influence of disinfection technologies (both novel and conventional) and emerging contaminants on DBP formation and toxicity are also needed in order to better navigate the rapidly changing water treatment landscape while mitigating potential adverse impacts on human and environmental health. To help meet these requirements, this dissertation compiled the findings of three interrelated studies assessing the roles of different disinfectant and microcontaminant regimens on the production of regulated DBPs and *in vitro* cytotoxic effects in a mammalian cell line (CHO cells) and a variety of relevant human cell lines (i.e. kidney, stomach, and colon).

As a whole, these results paint a reasonable picture of how different disinfectants and NPs impact DBP production in drinking water matrixes and their subsequent cytotoxic effects. Data from the chemical analyses (Sections 2.3.1., 3.3.1., 4.3.1.) show that only the synthetic waters disinfected with chlorine produced any regulated DBP concentrations, directly corresponding with past literature trends which show Fe(VI) as a DBP-free oxidizer. Data from the CHO-K1 and CaCo-2 cell viability assays (Sections 2.3.2, 3.3.2) show that none of the samples produced any significant alterations in cytotoxicity levels among the chosen cell lines. Data from the HEK-293, GES-1, and FHC cell viability assays (Section 4.3.2) show that samples disinfected with Fe(VI) were significantly less cytotoxic to a specific human cell line (HEK293) when compared to samples disinfected by chlorine. One of the more surprising outcomes from these assays showed that ZnO-dosed samples produced a significant decrease in HEK-293 cell cytotoxicity levels despite the chlorination of all NP-dosed waters. Though unexpected, the compound's photocatalytic oxidative properties may have outweighed any adverse effects stemming from the presence of DBPs. Regarding data from the ROS assays (Section 4.3.3), exposure to samples disinfected with higher concentrations of ferrate(VI) produced a significant increase in ROS generation among GES-1 cells. Exposure to ZnO-dosed samples also produced significant increases in ROS generation among GES-1 and FHC cells. Due to their high cellular viability, however, these increases in ROS are likely indicative of a generalized defensive response in the examined cells as opposed to the outcome of a legitimate toxic mechanism. Lastly, data

from the autophagy assays (Section 4.3.4) show that none of the extracts enhanced AVO accumulation among HEK293 cells, indicating low overall levels of cellular stress.

The results of these studies are subject to a number of limitations. Generating synthetic drinking water with DBP precursor concentrations that reflect idealized (i.e. highly dilute) national averages allowed for a high degree of reproducibility in generating water samples. They do not, however, encompass real world conditions which frequently surpass these levels. As such, the rate of DBP production and any subsequent cytotoxic effects may have been extremely subdued compared to those seen in many stressed/marginal-quality water resources throughout the country. Other limitations included a lack of detailed nanoparticle characterizations for each of the NP-dosed samples, and the exclusion of two regulated DBPs – bromate and chlorite – and other common non-regulated DBPs as part of the chemical analyses.

Even so, the findings from these studies provide useful observations that may aid in the reduction or elimination of DBPs in potable drinking water resources. They provide additional evidence that ferrate(VI) has real potential as an alternative to chlorination which would lower DBP formation in water treatment facilities. They illustrate the effects of ENMs on DBP production and toxicity, particularly the role of ZnO in certain human cell lines. Finally, these data offer direct cytotoxic comparisons between a variety of different cell lines. They indicate a higher degree of cytotoxic sensitivity among CaCo-2 and HEK293 when compared to the CHO-K1, GES-1, and FHC cell lines, as well as a higher sensitivity to ROS generation among GES-1 and FHC when compared to the HEK293 cell line. There are still many paths forward in assessing

how novel disinfection technologies or emerging contaminants impact the production/toxicity of unknown DBP mixtures. Potential avenues for future research projects in this area include similar analyses of synthetic water samples using DBP precursor concentrations that reflect contaminated or marginal-quality waters; similar analyses using more concentrated dilution levels (e.g. 80x REF); in-depth characterizations of NOM and NP interactions (e.g. how photocatalytic oxidative properties might balance out DBP toxicity); and the use of bioassay directed fractionation to delineate the toxicities of specific components in complex DBP mixtures.

As the body of literature progresses in new and exciting directions, researchers continually lay the groundwork for novel methods and technologies that could potentially limit and/or circumvent the production of DBPs and other toxic water-borne contaminants. By securing the safety of potable water resources and maximizing their usage, these tools (and the research that led to their development) will be instrumental in preserving public health in a water-strained future.

APPENDIX A

FIGURES

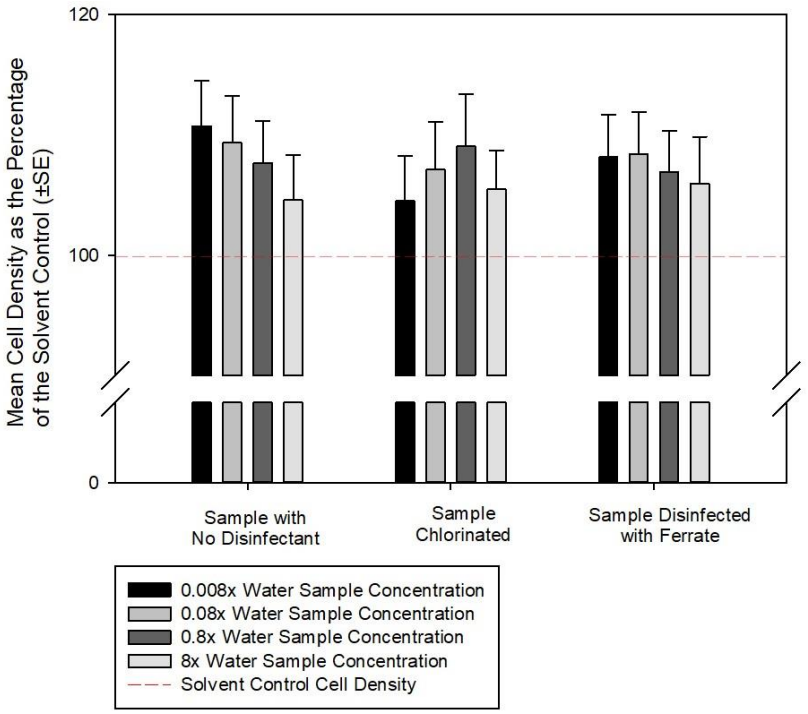

Figure A.1 Chronic CHO cell cytotoxicity: Assay results for samples treated with different disinfectants. Values indicate a percentage of the mean recorded cell density for each sample type as compared to the baseline cell density (100%) of the solvent control. A star (*) denotes that the difference in mean values among the indicated disinfectant group is statistically significant compared to the corresponding control group. Factoring in the extract type and dilution level separately, both terms show no significant effect on cell density (P = 0.839; P = 0.762). The interactive effects of the extract type and the dilution level on cell density are not statistically significant (P = 0.990).

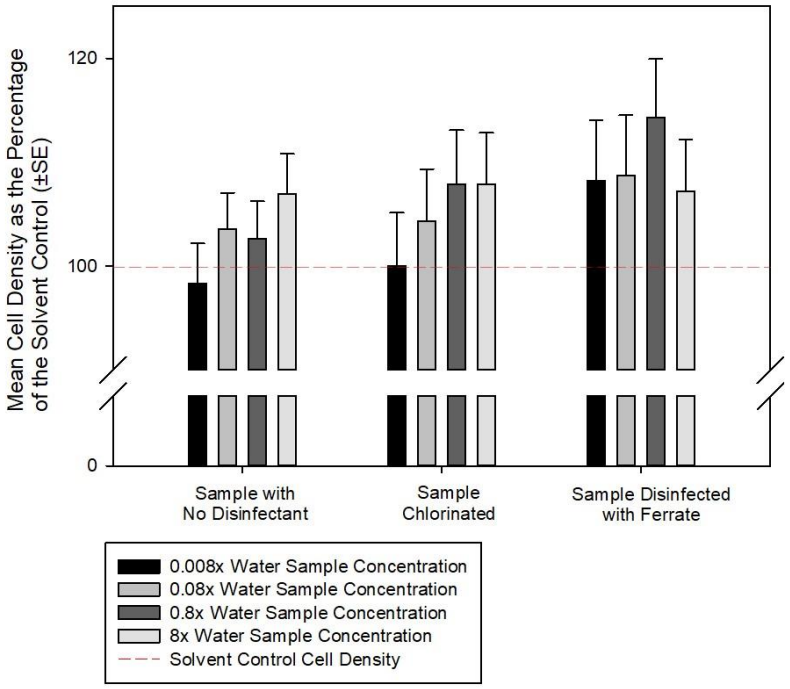

Figure A.2 Chronic cytotoxicity for CaCo-2 cells treated with different disinfectant extracts. Values indicate a percentage of the mean recorded cell density for each sample type as compared to the baseline cell density (100%) of the solvent control. A star (*) denotes that the difference in mean values among the indicated disinfectant group is statistically significant compared to the corresponding control group. A two-way ANOVA with interacting terms showed a statistically significant effect on cell density when factoring for extract type on its own (P = 0.005). However, when factoring for dilution level and the interacting effect of these two terms, no significant effects were found (P = 0.065; P = 0.538).

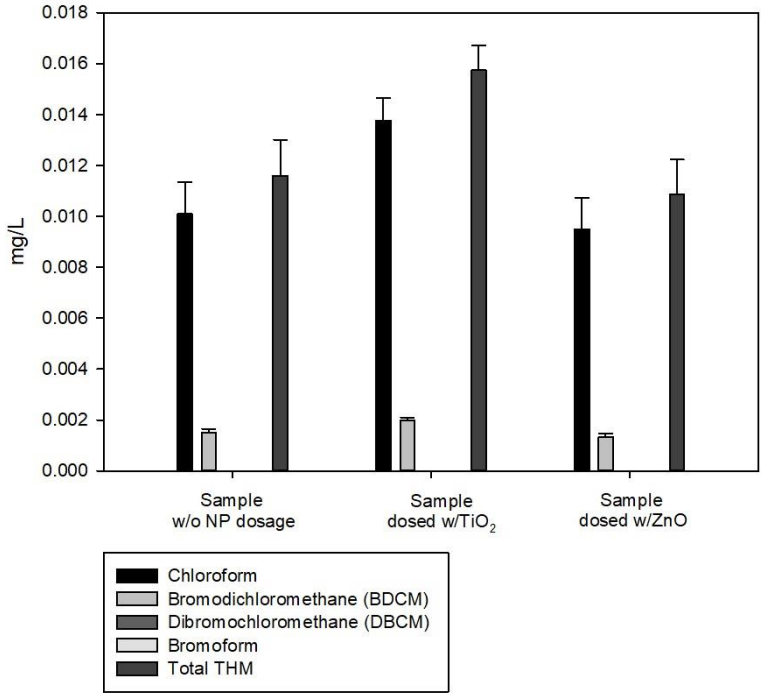

Figure A.3 Effect of nanoparticles on trihalomethane concentrations: chemical analysis results showing the occurrence of regulated trihalomethanes (mg/L) in synthetic drinking water samples dosed with different nanoparticles (TiO2 or ZnO). Disinfection byproduct (DBP) analysis of THMs was accomplished via gas chromatography/mass spectrometry (GC/MS) determination. All THM analyses were conducted according to EPA Method 524.2. The minimum reporting limit (MRL) was 1-2 ng/L. Differences in the mean values among the different sample types was not statistically significant (P = 0.799).

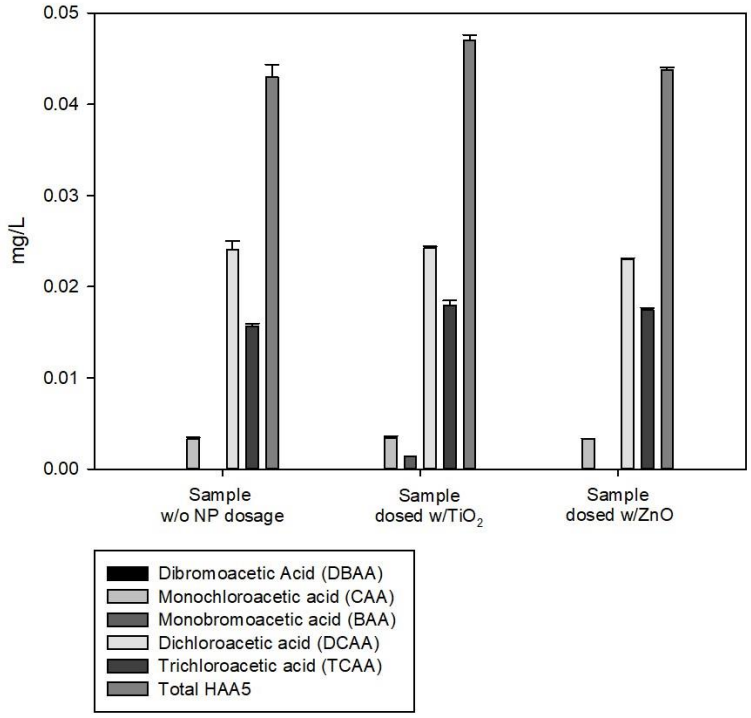

Figure A.4 Effect of nanoparticles on haloacetic acid concentrations: chemical analysis results showing the occurrence of regulated haloacetic acids (mg/L) in synthetic drinking water samples dosed with different nanoparticles (TiO2 or ZnO). Disinfection byproduct (DBP) analysis of HAAs was accomplished via gas chromatography/mass spectrometry (GC/MS) determination. All HAA analyses were conducted according to EPA Method 552.1. The minimum reporting limit (MRL) was 1-2 ng/L. The difference in mean values among the different sample types was not statistically significant (P = 0.851).

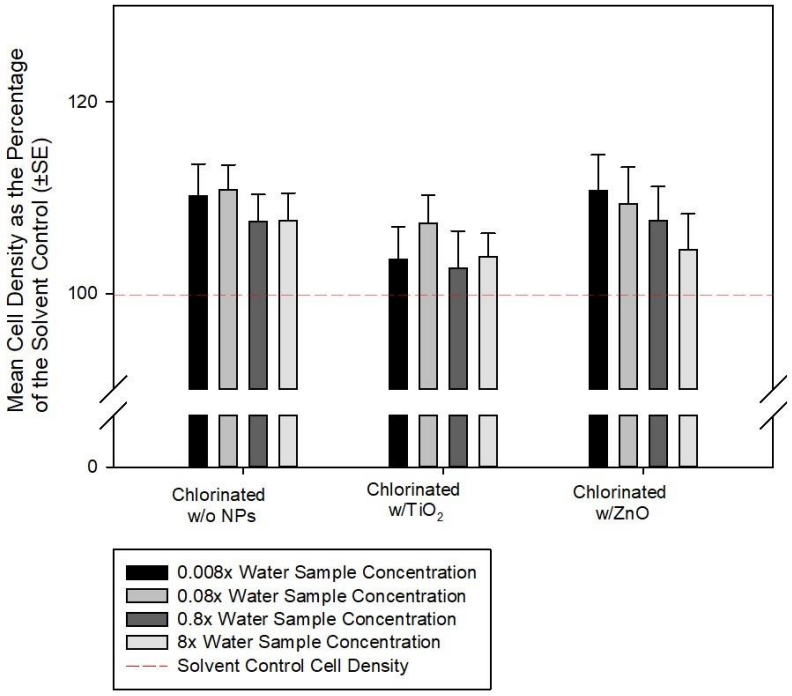

Figure A.5 Chronic cytotoxicity assay results for CHO cells exposed to nanoparticle extracts. Chronic cytotoxicity assay results in Chinese hamster ovary (CHO) cells exposed to water extracts from synthetic water samples dosed with different types of nanoparticles (no dosage, TiO_2, or ZnO). Values indicate a percentage of the mean recorded cell density for each sample type as compared to the baseline cell density (100%) of the solvent control. A star (*) denotes that the indicated sample type produced a significant change in cell density compared to the control at the corresponding dilution level. A two-way ANOVA with interacting terms showed a statistically significant effect on cell density when factoring for extract type on its own (P = 0.002). However, when factoring for dilution level and the interacting effect of these two terms, no significant effects were found (P = 0.067; P = 0.781).

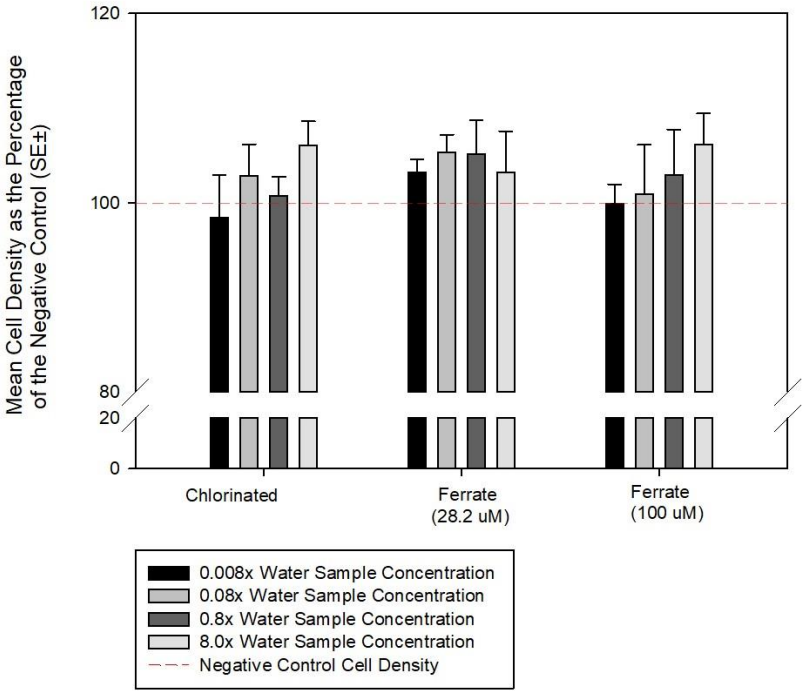

Figure A.6 Cell viability assay for GES-1 cells exposed to disinfectant extracts. Cell viability assay results from human gastric epithelial (GES-1) cells exposed to water extracts from synthetic water samples treated under different disinfectant and microcontaminant regimens. Values indicate a percentage of the mean recorded cell density for each sample type as compared to the baseline cell density (100%) of the solvent control. A star (*) denotes that the difference in mean values among the indicated disinfectant concentration group is statistically significant compared to the corresponding control concentration group. A One-way ANOVA showed no statistical significance (P = 0.171).

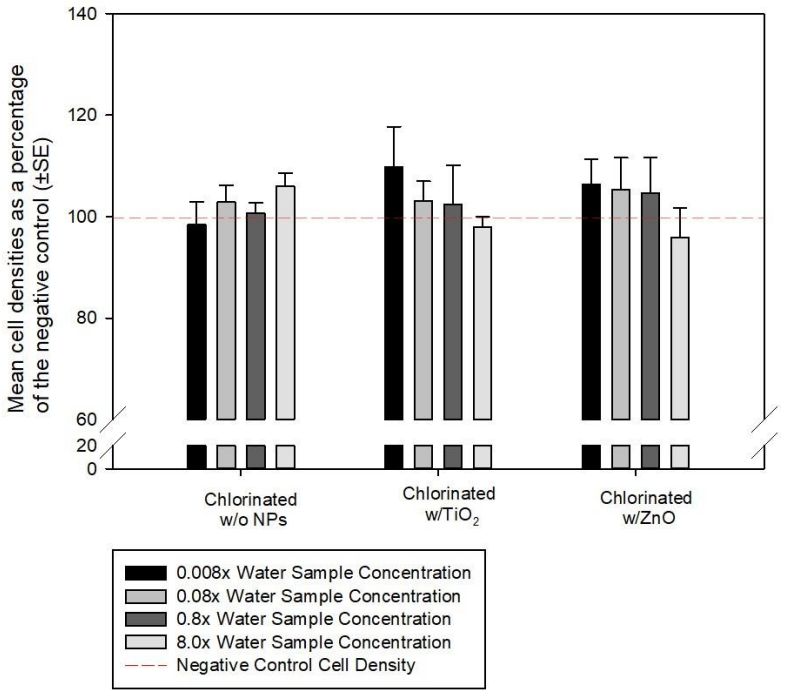

Figure A.7 Cell viability assay for GES-1 cells exposed to nanoparticle extracts. Cell viability assay results from human gastric epithelial (GES-1) cells exposed to water extracts from synthetic water samples treated under different disinfectant and microcontaminant regimens. Values indicate a percentage of the mean recorded cell density for each sample type as compared to the baseline cell density (100%) of the solvent control. A star (*) denotes that the difference in mean values among the indicated disinfectant group is statistically significant compared to the control group of its corresponding concentration. A one-way ANOVA showed that the difference in the mean values among the different extract types is not statistically significant (P = 0.118).

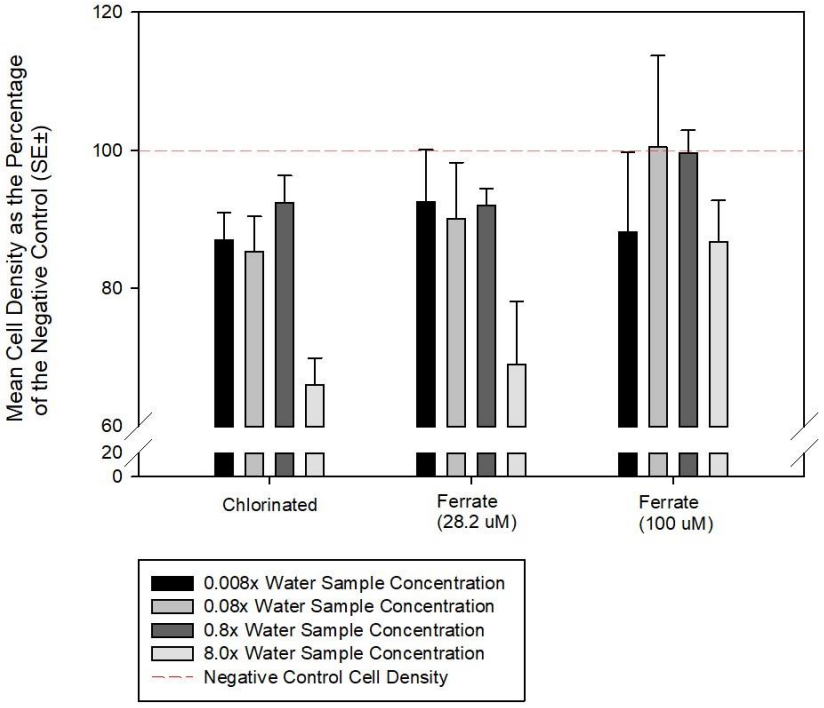

Figure A.8 Cell viability assay for FHC cells exposed to disinfectant extracts. Cell viability assay results from human fetal colon (FHC) cells exposed to water extracts from synthetic water samples treated under different disinfectant and microcontaminant regimens. Values indicate a percentage of the mean recorded cell density for each sample type as compared to the baseline cell density (100%) of the solvent control. A star (*) denotes that the difference in mean values among the indicated disinfectant group is statistically significant compared to the control group with a corresponding concentration. A one-way ANOVA showed that the difference in the mean values among the different extracts is statistically significant (P = <0.001). However, a pair-wise multiple comparison (Bonferroni t-test) revealed that none of the extracts are statistically significant compared to their corresponding control concentrations.

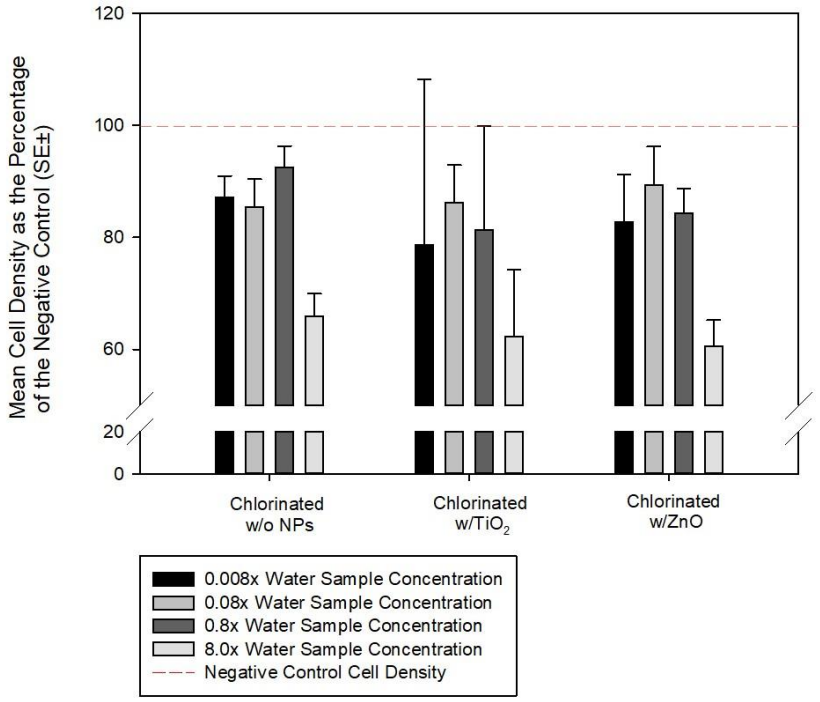

Figure A.9 Cell viability assay for FHC cells exposed to nanoparticle extracts. Cell viability assay results from human fetal colon (FHC) cells exposed to water extracts from synthetic water samples treated under different microcontaminant regimens. Values indicate a percentage of the mean recorded cell density for each sample type as compared to the baseline cell density (100%) of the solvent control. A star (*) denotes that the difference in mean values among the indicated disinfectant group is statistically significant compared to the control with a corresponding concentration. A one-way ANOVA showed the difference in the values among the different extract types is statistically significant (P = 0.028). However, a pair-wide multiple comparison (Bonferroni t-test) indicated that no concentration levels were statistically significant compared to their corresponding control.

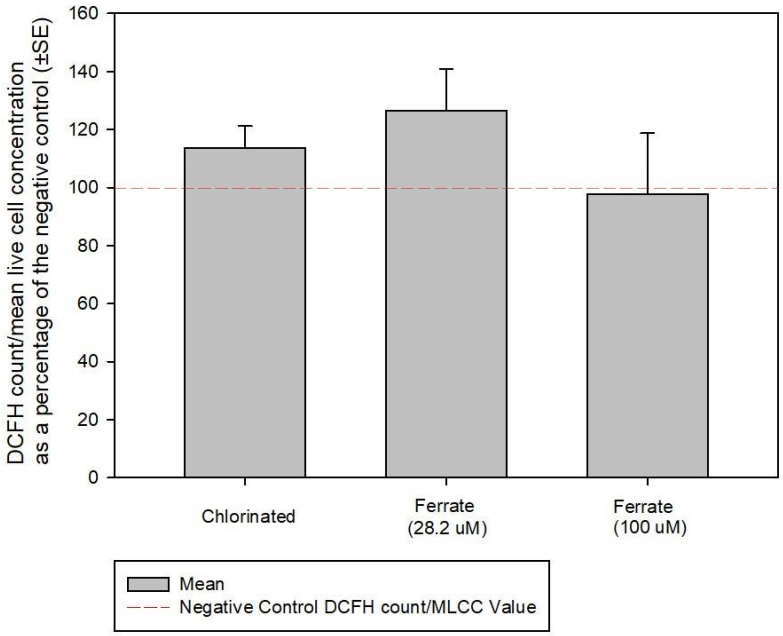

Figure A.10 ROS assay for HEK293 cells exposed to disinfectant extracts. ROS assay results from human kidney (HEK293) cells exposed to water extracts from synthetic water samples treated under different disinfectant regimens. Values indicate a percentage of the mean recorded cell density for each sample type as compared to the baseline cell density (100%) of the negative control. A star (*) denotes that the difference in mean values among the indicated disinfectant group is greater than would be expected by chance. A one-way ANOVA revealed that the differences in the mean values among the extract types are not statistically significant (P = 0.149).

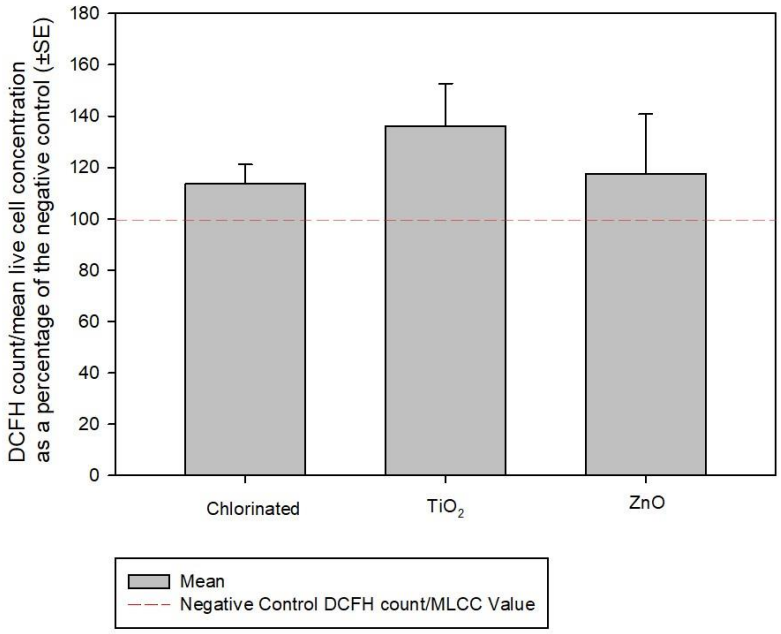

Figure A.11 ROS assay for HEK293 cells exposed to nanoparticle extracts. ROS assay results from human kidney (HEK293) cells exposed to water extracts from synthetic water samples treated under different microcontaminant regimens. Values indicate the mean recorded ratio between DCFH count/mean live cell concentration (MLCC) as a percentage of the negative control value (100%) of the negative control. A star (*) denotes that the difference in mean values among the indicated disinfectant group is greater than would be expected by chance. A one-way ANOVA revealed that the differences in the mean values among the extract types are not statistically significant (P = 0.304).

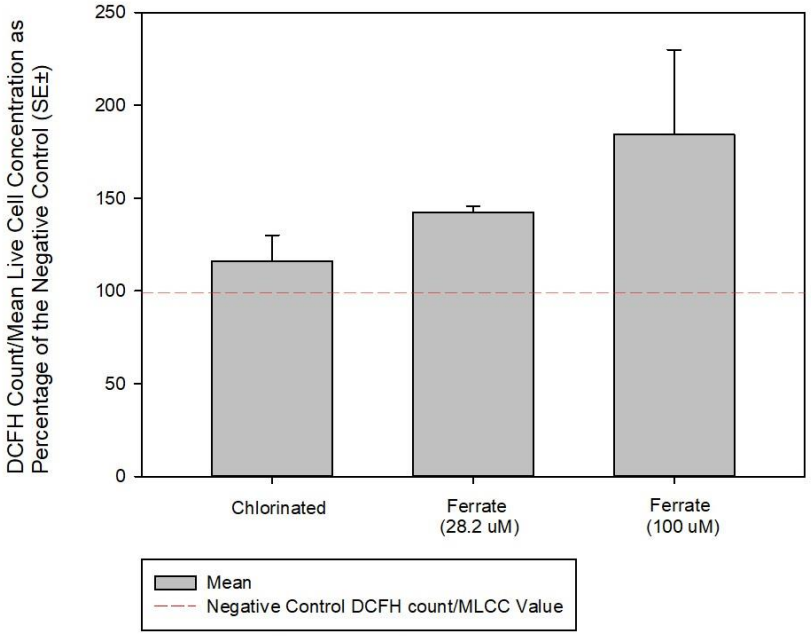

Figure A.12 ROS assay for FHC cells exposed to disinfectant extracts. ROS assay results from human fetal colon (FCH) cells exposed to water extracts from synthetic water samples treated under different disinfectant regimens. Values indicate a percentage of the mean recorded cell density for each sample type as compared to the baseline cell density (100%) of the negative control. A star (*) denotes that the difference in mean values among the indicated disinfectant group is greater than would be expected by chance after allowing for differences in REF level. A one-way ANOVA revealed that the differences in the mean values among the extract types are not statistically significant (P = 0.061).

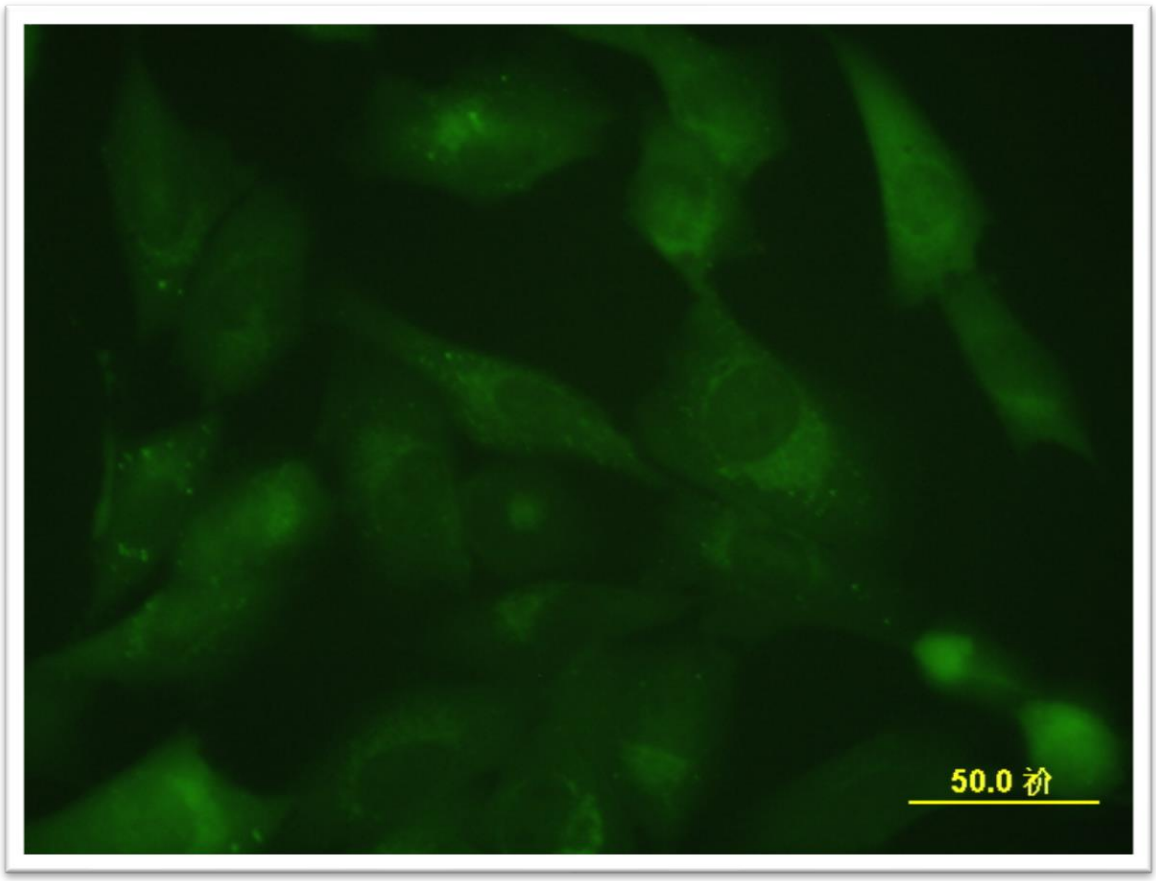

Figure A.13. Fixed HEK293 cells with florescent markers that identify the cytoplasmic sites of AVO accumulation after exposure to extracts from chlorinated drinking water.

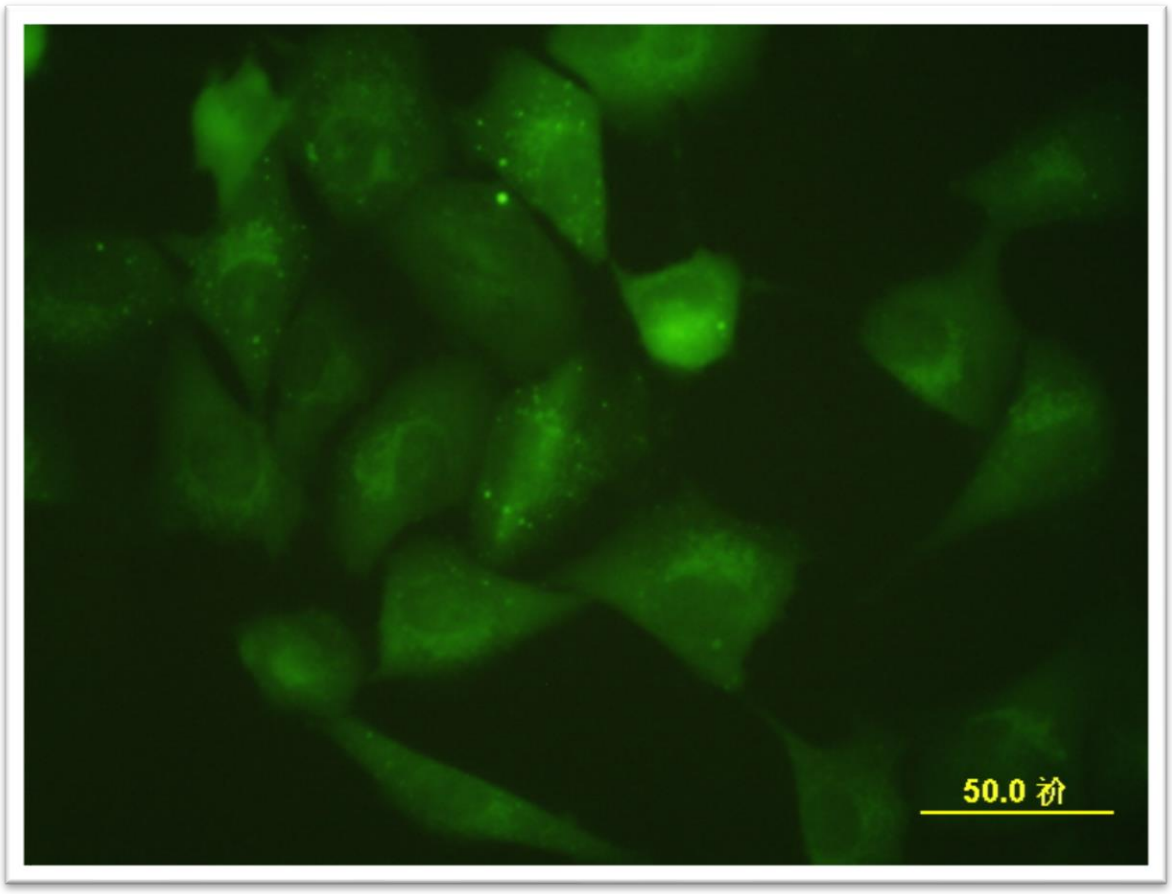

Figure A.14 Fixed HEK293 cells with florescent markers that identify the cytoplasmic sites of AVO accumulation after exposure to extracts from drinking water disinfected with 28.2 uM ferrate(VI).

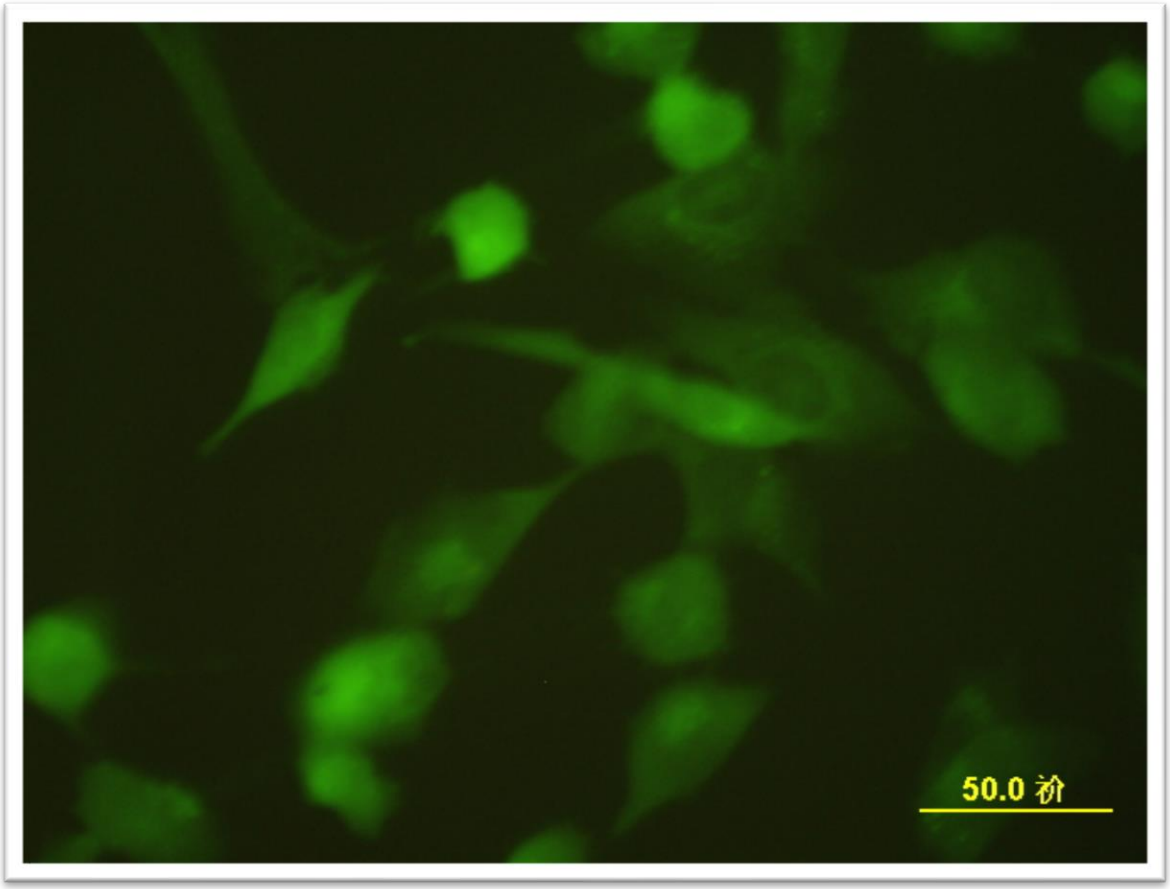

Figure A.15 Fixed HEK293 cells with florescent markers that identify the cytoplasmic sites of AVO accumulation after exposure to extracts from drinking water disinfected with 100 uM ferrate(VI).

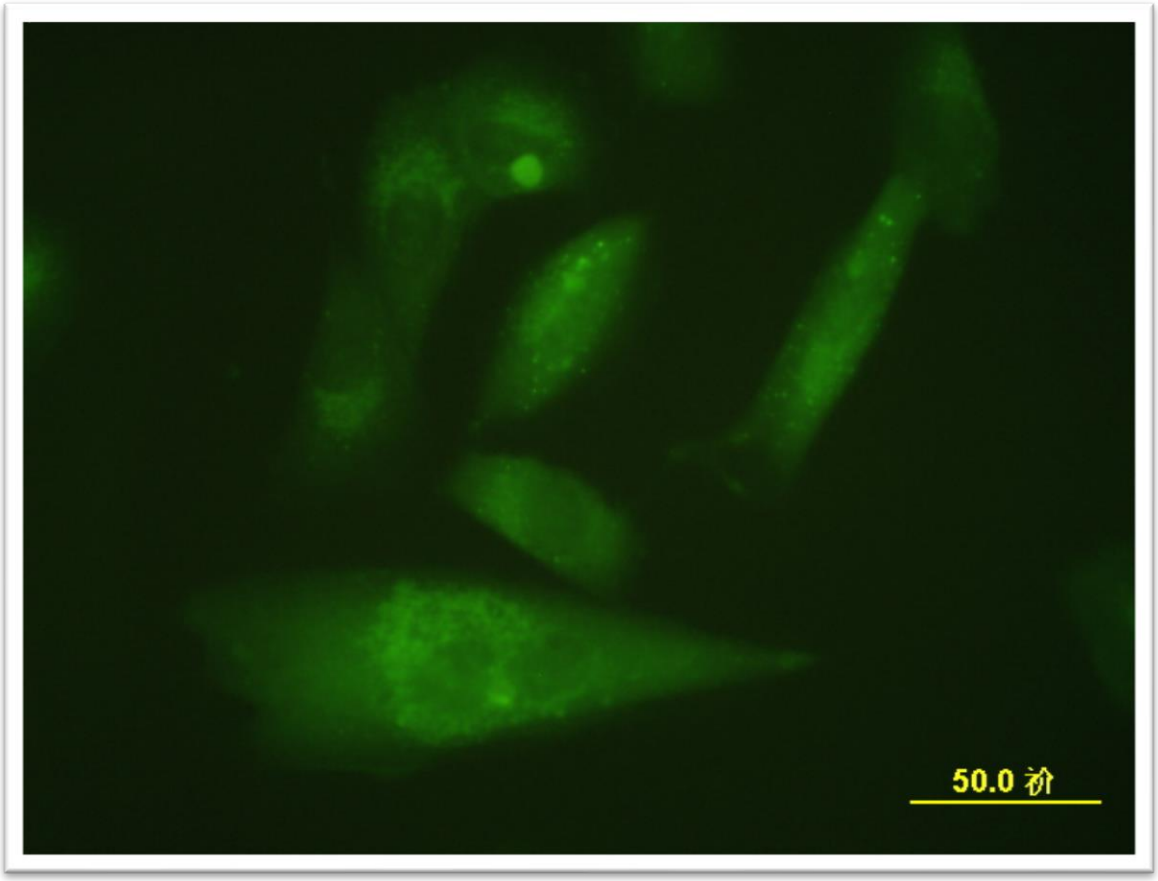

Figure A.16 Fixed HEK293 cells with florescent markers that identify the cytoplasmic sites of AVO accumulation after exposure to extracts from drinking water dosed with TiO_2.

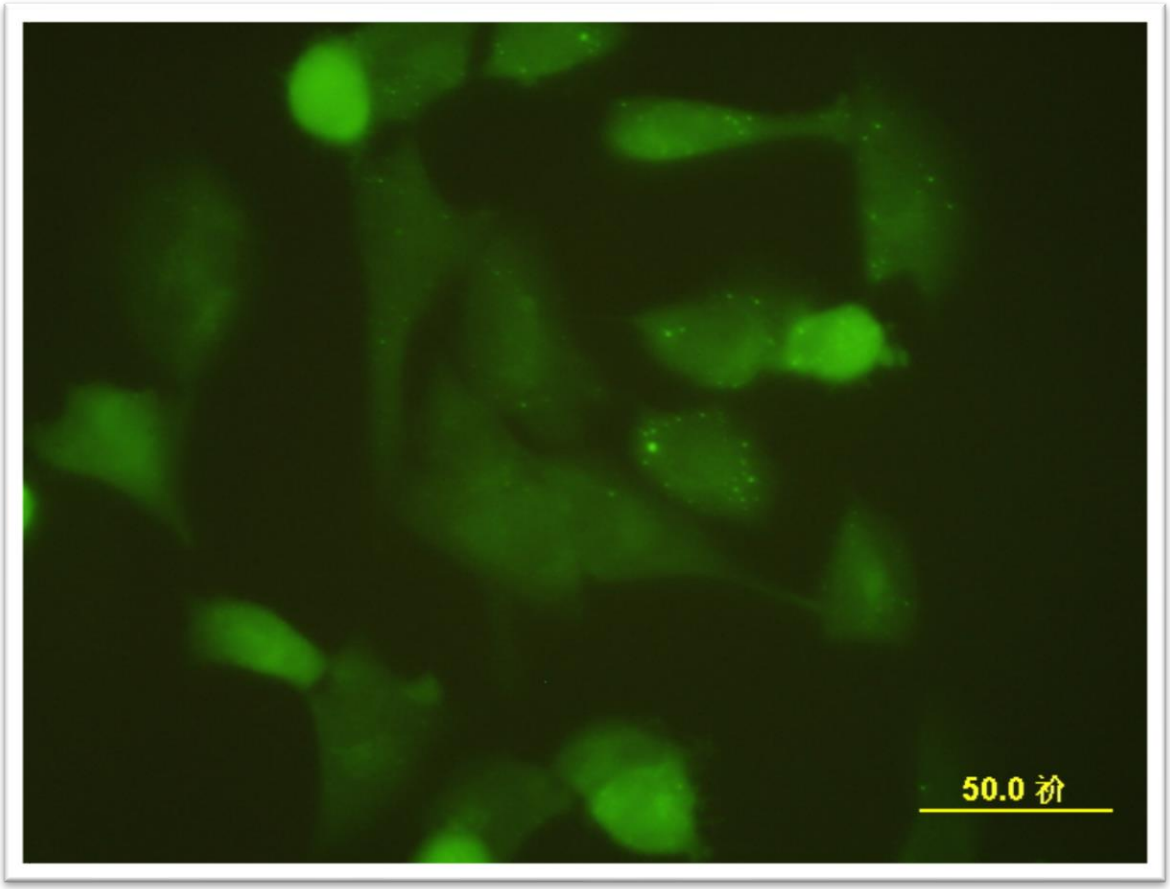

Figure A.17 Fixed HEK293 cells with florescent markers that identify the cytoplasmic sites of AVO accumulation after exposure to extracts from drinking water dosed with ZnO.

APPENDIX B

TABLES

Table 1: Chemical/Compound Information

Chem/Compound Name	Supplier	Supplier Cat. No.	CAS No.	Purity
Acetone	SIGMA-ALDRICH	270725-1L	67-64-1	≥99.9%
Crystal Violet	Fisher	C581-100	548-62-9	Reagent Grade
Dimethylsulfoxide (DMSO)	ATCC	4-X	67-68-5	≥99.5%
Dimethylsulfoxide (DMSO)	SIGMA-ALDRICH	D4540-500ML	67-68-5	≥99.5%
Eagle's Modified Essential Media (EMEM)	ATCC	30-2003	N/A	Reagent Grade
Erythrosin B	SIGMA-ALDRICH	198269-25G	15905-32-5	Reagent Grade
Ethanol 70%	VWR	E505-4L	64-17-5	Biotech Grade
Fetal Bovine Serum	ATCC	30-2020	N/A	Reagent Grade
Hexane	SIGMA-ALDRICH	650552-4L	110-54-3	≥95%
Hydrochloric acid 1.0N	VWR	BDH7202-1	7647-01-0	Reagent Grade
MES Hydrate	Alfa Aesar	H56472	4432-31-9	99+%
Methanol	SIGMA-ALDRICH	34860-4L-R	67-56-1	≥99.9%
Nitric Acid	VWR	BDH3046-2.5L	7697-37-2	Reagent Grade
Nutrient Mixture F-12 Ham	SIGMA-ALDRICH	N3520-10X1L	N/A	Reagent Grade
Penicillin-Streptomycin	SIGMA-ALDRICH	P4333-100ML	N/A	Reagent Grade
Phosphate Buffered Saline pH 7.2 (1X)	Gibco	20012-027	N/A	Reagent Grade
Potassium Bromide	Alfa Aesar	A16339	2139626	99+%
Potassium Iodide	Acros Organics	373651000	7681-11-0	99+%
Potassium Phosphate Monobasic	SIGMA-ALDRICH	795488-500G	7778-77-0	≥99%
Sodium Bicarbonate	SIGMA-ALDRICH	792519-500G	144-55-8	≥99.7%
Sodium Hydroxide 1.0N	VWR	BDH7222-1	1310-73-2	Reagent Grade
Sodium Hydroxide	SIGMA-ALDRICH	S5881-1KG	1310-73-2	≥98%
Sodium Hypochlorite Solution	SIGMA-ALDRICH	425044-250ML	7681-52-9	Reagent Grade

Sodium Phosphate Dibasic Heptahydrate	SIGMA-ALDRICH	RES0971S-A702X	7782-85-6	Pharma Grade
Sodium Sulfate	VWR	BDH9302-500G	7757-82-6	≥98%
Suwannee River Fulvic Acid	IHSS	2S101F	N/A	N/A
Titanium(IV) Oxide	SIGMA-ALDRICH	718467-100G	13463-67-7	≥99.5%
Trypsin-EDTA Solution	SIGMA-ALDRICH	T4049-500ML	N/A	BioReagent Grade
Zinc Oxide	SIGMA-ALDRICH	721077-100G	1314-13-2	≥99.5%

Table 2: Autophagy Assay Results

Sample Type	**Punctuates/Cell**
Control (Chlorinated)	2.70
Ferrate (28.2 uM)	3.08
Ferrate (100 uM)	1.00
TiO_2 NPs	2.42
ZnO NPs	3.45